Fluorinated benzylidene indanone exhibits antiproliferative activity through modulation of microtubule dynamics and antiangiogenic activity

Ankita Srivastava chemical synthesis ,
Kaneez Fatima Soft agar analysis; cell cycle; Antiangiogenesis; annexin V experiments ,
Eram Fatima chemical synthesis , Arjun Singh Acute oral toxicity ,
Aastha Singh chemical synthesis ,
Aparna Shukla Molecular docking studies ,
Suaib Luqman Soft agar analysis; cell cycle; Antiangiogenesis; annexin V experiments ,
Karuna Shanker Purity profile ,
Debabrata Chanda Acute oral toxicity ,
Feroz Khan Molecular docking studies ,
Arvind S. Negi Design & synthesis; manuscript preparation; overall planning; responsibility etc

PII: S0928-0987(20)30301-8
DOI: https://doi.org/10.1016/j.ejps.2020.105513
Reference: PHASCI 105513

To appear in: *European Journal of Pharmaceutical Sciences*

Received date: 3 May 2020
Revised date: 11 August 2020
Accepted date: 11 August 2020

Please cite this article as: Ankita Srivastava chemical synthesis , Kaneez Fatima Soft agar analysis; cell cycle; Anti
Eram Fatima chemical synthesis , Arjun Singh Acute oral toxicity , Aastha Singh chemical synthesis ,
Aparna Shukla Molecular docking studies , Suaib Luqman Soft agar analysis; cell cycle; Antiangiogenesis; annexi
Karuna Shanker Purity profile , Debabrata Chanda Acute oral toxicity , Feroz Khan Molecular docking studies ,
Arvind S. Negi Design & synthesis; manuscript preparation; overall planning; responsibility etc , Fluorinated benzylidene indanone exhibits antiproliferative activity through modulation of microtubule dynamics and antiangiogenic activity, *European Journal of Pharmaceutical Sciences* (2020), doi: https://doi.org/10.1016/j.ejps.2020.105513

Highlights

* An extensive cancer pharmacology of Fluorinated benzylidene indanone has been explored

* Induces late apoptosis in breast cancer cells (MCF-7 & MDA-MB-231)

* Occupies colchicine binding pocket of β-tubulin.

* Down-regulates tumour angiogenic factors; VEGF and HIF-α in MCF-7 cells.

* *In-vivo* efficacy: 48.2% tumour reduction at 120 mg/kg oral dose.

* Safety: *in-vivo* acute toxicity- safe up to 1000mg/kg dose

Fluorinated benzylidene indanone exhibits antiproliferative activity through modulation of microtubule dynamics and antiangiogenic activity

Ankita Srivastava,[a,b] Kaneez Fatima,[a,b] Eram Fatima,[a] Arjun Singh,[a] Aastha Singh,[a] Aparna Shukla,[a] Suaib Luqman,[a,b] Karuna Shanker,[a,b] Debabrata Chanda,[a,b] Feroz Khan,[a,b] Arvind S. Negi[a,b,*]

[a]*CSIR-Central Institute of Medicinal and Aromatic Plants (CSIR-CIMAP), Kukrail Picnic Spot Road, P.O. CIMAP, Lucknow-226015, India.*

[b]*Academy of Scientific and Innovative Research (AcSIR), Ghaziabad-201002, Uttar Pradesh, India.*

Abstract

The application of fluorine in drug design has been understood significantly by the medicinal chemists in recent years. Modulation of tubulin-microtubule dynamics is one of the most effective targets for cancer chemotherapeutics. A logically designed and identified lead compound, fluorinated benzylidene indanone **1** has been extensively evaluated for cancer pharmacology. It occupied colchicine binding pocket acting as microtubule destabilizer and induced a G2/M phase arrest in MCF-7 cells. Compound **1** exerted an antiangiogenic effect in MCF-7 cells by down-regulating Vascular Endothelial Growth Factor (VEGF) and Hypoxia Inducible Factor-α (HIF-α). In *in-vivo* efficacy in C3H/Jax mice mammary carcinoma model, benzylidene indanone **1** reduced tumour volumes by 48.2%. Further in acute oral toxicity studies compound **1** was well tolerated and safe up to 1000 mg/kg dose in Swiss albino mice. The fluorinated benzylidene indanone **1**, a new chemical entity (NCE) can further be optimized for better efficacy against breast adenocarcinoma.

Keywords: anticancer, breast cancer, benzylidene indanone, antitubulin, antiangiogenic, Ehrlich ascites carcinoma, toxicity.

*Corresponding author: E mail: arvindcimap@rediffmail.com (a.s. negi),
Tel: +91-522-2342676 x 583; Fax: +91-522-2342666;

1. Introduction

Breast cancer is the second most common cancer in the world. It is the most frequent cancer among women with an estimated 2.1 million new cancer cases diagnosed and 0.63 million deaths in 2018 [**Cancer: WHO factsheet 2018**]. It caused 0.57 million mortality in women which was more in less developed countries. Over the past two decades the survival rate of breast cancer patients has been enhanced significantly due to better diagnostic tools and more effective adjuvant therapies. In India, breast cancer (14%) was the most prevalent among all types of cancers [**Breast Globocon 2019**]. There are sufficient evidences that endogenous estrogens play a critical role in the development of breast cancer [**Nowsheen et al. 2012; Samavat et al. 2015**]. About two third of breast cancer cases are hormone dependent breast cancer also known as estrogen positive (ER+ve) breast cancer. The ER positive breast cancer is sensitive to hormone therapy and is commonly treated with estrogen antagonists and/or aromatase inhibitors [**Gupta et al. 2013**]. Traditionally, breast cancer treatment decisions are made based on tumour histology and status of three main biomarkers, ER (estrogen receptor), PR (progesterone receptor) and HER2 (erb-B2 receptor tyrosine kinase 2) [**Baselga et al. 2010**]. There are several clinical drugs being used alone or in combinations to tackle the disease. Raloxifene and tamoxifen as estrogen antagonists for preventive medicines, paclitaxel, docetaxel, and abraxane, albumin bound paclitaxel nanoparticles as microtubule stabilizers, anastrozole and exemestane as aromatase inhibitors, Doxorubicin as DNA topo-II inhibitor, 5-fluorouracil as antimetabolites, fulvestrant as estrogen receptor down-regulator, abemaciclib as CDK inhibitor, gefitinib as tyrosine kinase inhibitor, and several monoclonal antibodies like herceptin etc. However, due to the high degree of heterogeneity of breast tumours, multiple biomarkers for molecular profiling and diverse therapeutic treatment options are being explored.

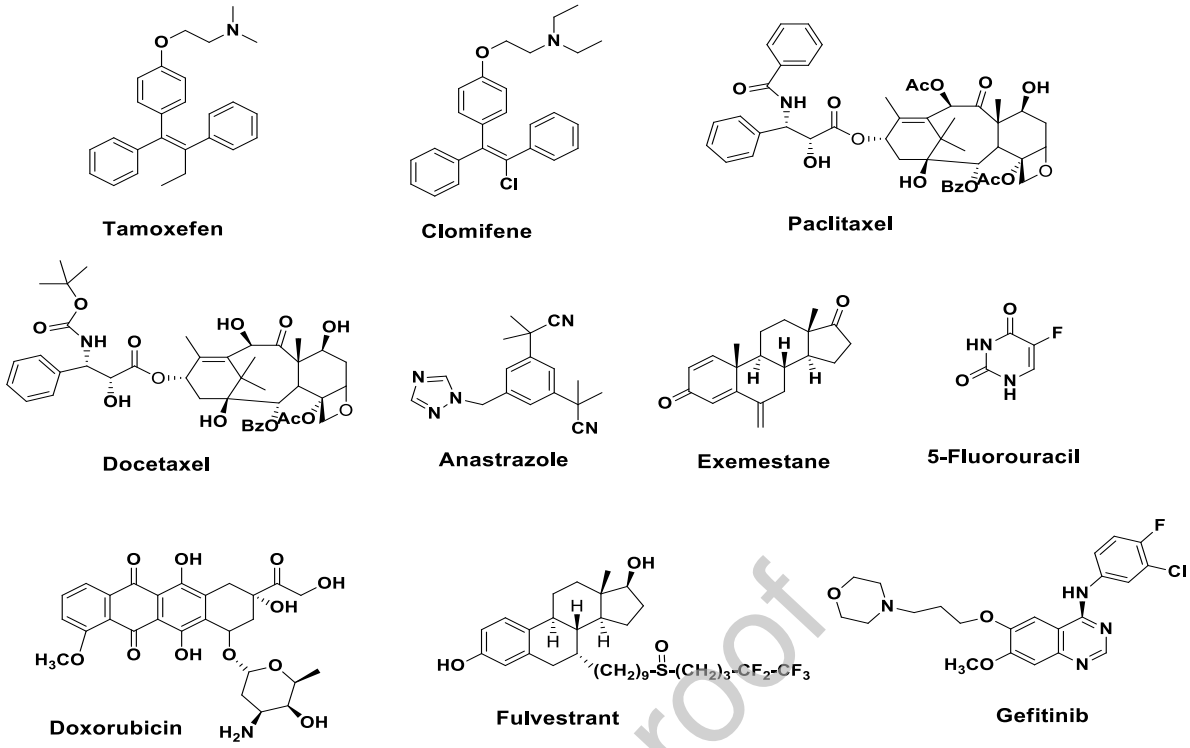

Figure 1: Some of the clinical drugs being used against breast cancer

Drugs that target tubulin and microtubule have been amongst the most successful modes of cancer chemotherapy [**Negi et al. 2015**, **Gan et al. 2007**]. Tubulin is a globular protein which exists as α/β dimeric form. Tubulin is polymerised to microtubule which plays an important role during mitosis in cell division. A dynamic equilibrium exists between soluble tubulin and tubulin in microtubules. Any interference in this process induces cell cycle arrest. Among the drugs that perturb microtubule functionare microtubule stabilizers like paclitaxel and epothilones and microtubule destabilizers such as colchicine, podophyllotoxin and combretastatins. There are several antitubulin drugs in clinical use and many more are under various phases of clinical trials.

Present communication deals with an antitubulin lead compound **1** belonging to arylidene-indanone class that was designed based on structure-activity relationship of several natural antitubulins. Arylidene indanone scaffold possesses various biological activities specifically anticancer activity [**JCJMDS Menezes 2017**]. Podophyllotoxin (PDT), colchicine and combretastatin A4 (CA4) are important microtubule destabilizers possessing a 3,4,5-trimethoxyphenyl fragment in their structures (Fig. 2). This fragment interacts with the β-tubulin and is responsible for their effects on microtubules. Based on these facts, we designed a hexamethoxy-2,3-diaryl-1-indanone pharmacophore containing ring A and this fragment as a possible antitubulin agent. Compound **1** is a fluorinated derivative of hexamethoxy-2,3-diaryl-1-indanone moiety.

Attributed to the potent *in-vitro* anticancer activity of compound **1**, its detailed pharmacology was explored systematically. Various experiments were performed to establish its cytotoxicity, mechanism of action and finally preclinical efficacy and toxicity in rodent models.

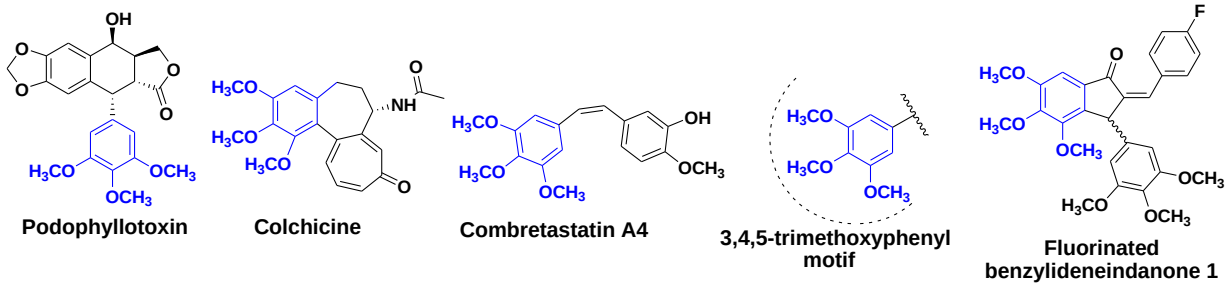

Fig. 2: Structures of naturally occurring microtubule destabilizers (PDT, colchicine and CA4) possessing 3,4,5-trimethoxyphenyl fragment, designed pharmacophore and fluorinated lead compound **1**.

2. Materials and methods

2.1 General

Melting points were determined in open glass capillaries and were uncorrected. Gallic acid was procured from S.d. Fine Chemicals India. Reagents and other chemicals were purchased either from Sigma-Aldrich, USA or Avra Synthesis India and used without purification. Reactions were monitored on Merck pre-coated silica gel TLC-GF_{254} aluminium sheets and visualization of compounds was done under UV light (254 nm and 365 nm) and further charring with 2% ceric sulphate in 10% sulphuric acid (aqueous). Purification of compound **1** was done on Flash chromatography system (CombiFlash R_f200i, Teledyne-ISCO, USA) using glass column (13 cm lengthx2 cm i.d.) and silica gel (230-400 mesh) using a UV detector (254 nm & 280 nm) and characterised by ^{1}H and ^{13}C NMR, ESI-MS, and ESI-HRMS. NMR spectra were obtained with Bruker Avance-500 MHz spectrometer. Chemical shifts are given in δ ppm values with respect to tetramethylsilane (TMS) as an internal standard. ^{1}H–^{1}H coupling constant (J) values are given in Hz. ESI mass spectra were recorded using an APC3000 LC-MS-MS (Applied Biosystem) and High Resolution Mass (HRMS) on Agilent 6520Q-TOF after dissolving the compounds in methanol.

DMEM (Dulbecco's Modified Essential Eagle Medium) and FBS (Fetal Bovine Serum) were purchased from Gibco (ThermoFisher, India). RNaseA, Crystal Violet Dye, HEPES, Trypsin-EDTA, Antibiotic-Antimycotic (Ab-Am) Solution, Phosphate Buffer Saline (PBS), Citric Acid and Propidium Iodide (PI) were acquired from Sigma-Aldrich, USA. Sodium bicarbonate ($NaHCO_3$), Agar, Sodium Citrate and Di-sodium Hydrogen Phosphate were obtained from Himedia Laboratories, India. Solvents including ethanol and isopropanol were procured from Merck, India Ltd.

2.2. Chemical synthesis

Compound **1** was synthesized from gallic acid as per our reported method [**Saxena et al. 2008**, **Prakasham 2012**].

The selected physical data;

3-(3',4',5'-trimethoxyphenyl)-4,5,6-trimethoxy-2-(4"-fluorobenzylidene)-indan-1-one (**1**)

Overall yield:14.29% (Six steps); M.P.:151-153^{o}C [156-158^{o}C, **11**]; TLC (Ethylacetate:Hexane=40:60): R_f=0.41; ^{1}H NMR ($CDCl_3$, 500MHz): δ 3.46 (s, 3H, OCH_3), 3.73 (s, 9H, 3xOCH_3), 3.91 (s, 3H, OCH_3), 3.94 (s, 3H, OCH_3), 5.26 (s, 1H, 3-CH), 6.43 (s, 2H, 2' & 6'-CH of 3-phenyl), 6.95-6.98 (t, 2H, 2" & 6"-CH of benzylidene ring, J=8.5Hz), 7.23 (s, 1H, 7-CH of indanone ring), 7.47-7.51(bs, 2H, 3" & 5"-CH of benzylidene ring), 7.66 (s, 1H, benzylidene-CH). ^{13}C NMR ($CDCl_3$, 75MHz): δ 46.15, 56.20, 56.31, 56.31, 60.29, 60.91, 60.94, 101.42, 105.89, 105.89, 115.44, 115.61, 130.56, 131.97, 133.03, 133.09, 133.37, 136.70, 136.81, 139.42, 139.44, 140.92, 148.78, 149.98, 153.04, 154.97, 162.21, 193.66. ESIMS (MeOH): 495 $[M+H]^+$, 517 $[M+Na]^+$; ESI-HRMS (CH_3CN): cacl for $C_{28}H_{28}FO_7$ $(M+H)^+$, 495.1819, found 495.1815.

2.3. UPLC analysis for purity profile

The purity profile was checked with a reverse phase Ultra Pressure Liquid Chromatography system (Waters USA) with Empower® software using a C-18 column (BEH130 Å, 1.7X 50 mm, 1.7 µm, Waters, USA, thermostated at 35±0.1 °C). Column analysis was performed with a using isocratic elution of Mobile phase Water (0.1% acetic acid): Acetonitrile in 40:60 (v/v) at flow rate of 0.2 mL/min. The injection volume was 2 µL. The integration on the peak area was performed at λ_{max} 325 nm. While, 3D chromatographic data acquisition in the range of 210-400 nm was done to monitor possible impurities under optimised analytical conditions. The purity was calculated by peak area normalization. Under optimised chromatographic condition, compound **1** was eluted at 1.817 min without interference of any neighbouring co-eluting peak. As a reference method, the PDA functions of UPLC software Empower® (Waters USA) were used to ensure the presence of a spectrally homogeneous peak.

2.4. Antiproliferative activity by soft agar colony assay

Human breast cancer cells, MCF-7 and MDA-MB-231 were seeded ($5x10^4$ cells per mL) separately in 24 well plates with or without compound **1** treatment for 24 h [**Kakuguchi et al. 2010**]. The bottom jelly layer was made with 0.72% agar and 4 mL media in a 60 mm petridish followed by the formation of the top layer consisting of cells and 3 mL media in 0.36% agar. Petridishes were

incubated in a CO_2 incubator for 15-20 days until the appearance of colonies followed by staining with Crystal Violet (0.04% in 2% ethanol) and incubated for 1h at RT. After the incubation period, colonies were counted using an inverted microscope and pictures were captured accordingly.

2.5. Cell cycle analysis

The effect of compound **1** on the cell division cycle of both MCF-7 and MDA-MB-231 cells under two independent experiments was assessed by two independent flow cytometry analysis using propidium iodide (PI) to stain cellular DNA [**Riccardi et al. 2006**]. Briefly, 2 x 10^6 cells per mL were grown in a 6 well plate at 37^{o}C in 5% CO_2 with or without compound **1** treatment for 24 h. After incubation, cells were collected and washed with PBS. Following removal of the PBS cells were fixed-in 70% ethanol added drop-wise while vortexing and left overnight at 4 ˚C. The fixed cells were centrifuged at high rpm to remove ethanol followed by washing with PBS and addition of DNA extraction buffer. The samples were incubated for 5 min at room temperature and centrifuged again to get a pellet. The pellet thus obtained was dissolved in PI staining solution followed by RNaseA (200 µg/mL) treatment and incubated for 30 min at RT. Finally, cell cycle analysis was done with a BD Biosciences LSR II flow cytometer (San Jose, CA, USA) and the analysis was performed using FACS Diva Software, version 6.1.3. Cell cycle experiments were performed in duplicates and results were expressed as Mean ± 1SD.

2.6. Apoptosis Vs Necrosis induction by 6a by Annexin V-FITC assay

For Annexin V-FITC apoptosis assay manufacturer's protocol was followed (BD Bioscience Kit). Two independent experiments were done for each MCF-7 and MDA-MB-231 on Flow cytometry [**Looi et al. 2013**]. 1 X 10^6 cells/mL cells (MCF-7 or MDA-MB-231) were seeded in 6-well plate and left overnight before treatment with compound **1** at various concentrations (at half IC_{50}, IC_{50} and $2xIC_{50}$) for 24 hours. All cells were collected and centrifuged at 5000 rpm for 5 min at 4 ºC and washed twice with cold PBS. Pellets were dissolved in 100 µL 1x binding buffer and incubated with 5 µL FITC-annexin-V and 5 µL propidium iodide (PI) for 15 min. Samples were resuspended in 500 µL 1x binding buffer and stained cells were analysed by FACS Diva software of flow cytometer within 1 h. The annexin V-FITC binds to phosphatidiylserine present on membrane surface in case of apoptotic cells whereas PI labels-cellular DNA in necrotic cells. This combination allows the differentiation among viable cells (annexin V negative, PI negative), early apoptotic cells (annexin V positive, PI negative), late apoptotic cells (annexin V positive, PI positive), and necrotic cells (annexin V positive, PI positive).

2.7. Molecular docking studies

The crystallographic structure of selected target β-Tubulin (PDB: 4O2B) was retrieved from protein databank (http://www.pdb.org). The structure of protein β-Tubulin and ligands colchicine, podophyllotoxin and compound **1** were prepared by using Autodock Tools v1.5.6 (MGL, La Jolla, USA). The tool converts protein structure into AD4 type then adds atomic partial charges, polar hydrogens and torsional degrees of freedom. The tool generates extended PDBQT file for protein and ligands. The grid parameter file and docking parameter files were prepared by setting grid centre at colchicine binding site with dimensions x= 13.686207, y= 8.663517 and z = -19.963483. The grid dimension was taken as x= 64, y=64 and z=64. AutoDock docking software used free energy force field and Lamarckian-Genetic algorithm to search stable conformation and binding free energy of ligand. For docking protocol optimization, a co-crystallised ligand redocking study was performed without randomizing ligand co-ordinates. Molsoft-chemist v3.8-6a 2018 was used for root mean square deviation (RMSD) value between redocked and β-Tubulin co-crystallised colchicine pose. Post docking analysis of protein-ligand complex was performed by using discovery studio v17.2.0.16349 visualizer.

2.8. Prediction of in-silico oral bioavailability and toxicity assessment

Here, the parameters for oral bioavailability for studied compounds were assessed through standard commercial and non-commercial tools namely TOPKAT (DS v3.5), Molsoft-chemist v3.8-6a (2018), SwissADME (http://www.swissadme.ch). TOPKAT use their patented QSTR models to predict ADME and toxicity for different endpoints *e.g.*, hepatotoxicity, CYP2D6 interaction, plasma-protein binding (PPB), blood-brain-barrier (BBB) penetration, carcinogenicity in rodents, Weight of Evidence (WOE) prediction, Ames mutagenicity, developmental toxicity, skin irritancy, skin sensitization, ocular irritancy, developmental toxicity and aerobic biodegradability etc. The TOPKAT prediction reliability is assessed by the software based benchmarked QSTR model optimal predictive space (OPS) applicability domain. Likewise, Molsoft and SwissADME used their benchmarked models to predict different ADME parameters.

2.9. Antiangiogenesis activity: a) Hypoxia Inducible Factor-1α

Hypoxia-inducible factor 1-alpha, a constitutively expressed transcription factor includes promotion of angiogenesis, responsible for tumor growth and its survival. The assay was carried out as per the described protocol of HIF-1α human ELISA Kit from Abcam (Catalog no. ab171577) [**Reen et al.**

2016, **Phelan et al. 2016**]. Briefly, 50 µL of standards and samples were pipetted into the appropriate well as described in the manual (cell lysate was prepared after giving 24 h treatment in MCF-7 cell line) followed by the addition of 50 µL of antibody cocktail to each well. The plate was incubated for an hour at room temperature on a shaker set to 400 rpm. After incubation the plate was washed with buffer (300 µL) and the liquid was completely removed by aspiration or decantation. 100 µL of tetramethylbenzidine (TMB) substrate solution was added to each well and the color was allowed to develop in a proportion to the amount of bound HIF-1α. The stop solution (100 µL) changed the color from blue to yellow and the intensity of the color was immediately measured at 450 nm. All samples were assayed in replicate (duplicate). Doxorubicin (1 µg/mL) was used as a standard inhibitor. The concentration of HIF-1α in the samples is then determined by comparing the optical density of the samples to the standard curve and the total protein content of sample was estimated by Nano Drop. The percent difference was calculated by comparing with control values.

b) Vascular Endothelial Growth Factor (VEGF)

Over-expression of vascular endothelial growth factor promotes tumor growth by formation of new blood vessels, a process known as angiogenesis. The vascular endothelial growth factor (VEGF) assay was carried out as per the described protocol in VEGF human ELISA kit from Abcam (Catalog no. ab100663) [**Petrica et al., 2017**]. Briefly, this assay employs an antibody specific for human VEGF coated on a 96 well plate. 100 µL of standards and samples were pipetted into the appropriate wells as per the manual description (cell lysate was prepared after giving 24h treatment in MCF-7 cell line) and the samples having VEGF bound to immobilized antibody (Lihui *et al.* 2006). After washing with buffer (300 µL) the liquids from the wells were completely removed by aspiration or decantation. Then 100 µL of 1X biotinylated antibody specific to VEGF was added and the plate was incubated for an hour followed by washing to remove unbound biotinylated antibody. 100 µL of streptavidin conjugated horse radish peroxidase (HRP) was added into each well and allowed to leave it for 45 min. The wells were again washed and 100 µL of tetramethylbenzidine (TMB) substrate solution was added to the wells and the color developed is in proportion to the amount of bound VEGF. The stop solution (50 µL) changed the color from blue to yellow and the intensity of the color was measured at 450 nm immediately. All the samples were assayed in replicate. Doxorubicin (1 µg/mL) was used as a standard inhibitor. The concentration of VEGF in the samples is then determined by comparing the optical density of the samples to the standard curve and the total protein content of sample was estimated by Nano Drop. The percent difference was calculated and compared with control values.

2.10. *In vivo* anticancer activity of compound 1 against mice mammary carcinoma

The *in-vivo* anticancer efficacy assay was performed against C3H/Jax mice mammary carcinoma model at ACTREC, Mumbai, India. The experiment was approved by Institute's Animal Ethical Committee (IAEC) *via* approval No. 01-2015. Inbred C3H/Jax mice were obtained from Institute's (ACTREC Mumbai) animal colony. The mammary tumour incidence in virgin females is 6-70%. Thirty six female mice of body weight 24±3 g each were used in the study. The temperature of the animal colony was maintained at 21±1^{o}C and humidity at 50-60% and a 12 h light/dark cycle was used. All the animals were fed *ad libitum* with standard laboratory diet. Five groups, each consisting of six randomly chosen animals, were used in this assessment. Group I was kept as control group (no treatment), Group II was for positive control (drug) Adriyamycin (Doxorubicin) at 2.5 mg/kg *i.v.* on day 1, 5, 9. Group III-V were treatment groups with compound **1** at 30 mg/kg, 60 mg/kg and 120 mg/kg orally 5 days a week for four weeks respectively, Compound **1** was dissolved in 1% DMSO in water and gavaged orally. This concentration of DMSO is not considered toxic to animals. The control group mice received the only vehicle.

The body weight, tumour volume, % survival were observed. Relative tumour volume (RTV) and T/C ratio were calculated;

Control groupmiceweregiveneither1%DMSO in PBS oral gavage or PBS intraperitoneal injection alone

RTV=Tumour volume on day of measurement/Tumour volume on day 1

T/C (Activity criteria) = Relative tumour volume of mice receiving test compound/Relative tumour volume of control animals

In-vivo efficacy of compound **1** was evaluated against C3H/Jax mice mammary tumour model taking Nod/Scid mice strain. Five different groups were taken six mice in each group (n=6), one control, one standard drug and three test groups.

A) Control

B) Positive control: Doxorubicin (Adriyamycin)-2.5mg/kg *i.v.* injection on 1, 5, and 9 days.

C) Compound **1**: 20mg/kg oral gavaging 5days a weekx4 weeks

D) Compound **1**: 40mg/kg oral gavaging 5days a weekx4 weeks

E) Compound **1**: 80mg/kg oral gavaging 5days a weekx4 weeks

Animals were exposed to drug for four weeks and- were sacrificed on the 29th day. Tumour volumes were calculated by assuming that the shape of a tumour approximated that of a sphere: Volume of sphere, $V= (4\pi/3)\ r^3$; average diameter $d=(d_1+d_2)/2$

$V= (\pi/6)\ d^3$; volume obtained was divided by 1000 to convert mm^3 to cm^3.

$$\% \text{ tumour reduction} = \frac{\text{Relative tumour volume of control (A) - Relative tumour volume of test}}{\text{Relative tumour volume of control (A)}} \times 100 ;$$

$$\text{and T/C} = \frac{\text{Relative tumour volume of test group}}{\text{Relative tumour volume of control (A)}}$$

2.11. *In-vivo* safety studies by acute oral toxicity

In view of potent anti-cancer activity of compound **1** in *in-vitro* model, its safety profiling was done *via* acute oral toxicity in Swiss albino mice. Experiment was conducted in accordance with the Organization for Economic Co-operation and Development (OECD) test guideline No 423 (1987). The study and number of animals used were approved by the Institutional Animal Ethics Committee (IAEC) of CSIR-Central Institute of Medicinal and Aromatic Plants, Lucknow, India *via* CIMAP/IAEC/2016-19/1 dated 09-02-2017.

For the acute oral toxicity experiment, 30 mice (15 male and 15 female) were taken and divided into four groups comprising 3 male and 3 female mice in each group (body weight=20-25 g each). The animals were maintained at 22±5 ^{0}C with humidity control and also on an automatic dark and light cycle of 12 hours. The animals were fed with the standard mice feed and provided *ad libitum* drinking water. Mice of group 1 were kept as control and animals of groups 2, 3, 4, and 5 were kept as experimental. The animals were acclimatized for 7 days in the experimental environment prior to the actual experimentation. The test compound **1** was dissolved in a minimum volume of dimethylsulphoxide, suspended in caboxymethylcellulose (0.7%) and was given at 5, 50, 300 and 1000 mg/kg body weight to animals of groups 2, 3, 4 and 5 respectively. Control animals received only vehicle.

Observational, haematological, biochemical and gross pathological study

Animals were checked for mortality and any signs of ill health at hourly interval on the day of administration of drug and thereafter a daily general case side clinical examination was carried out including changes in skin, mucous membrane, and eyes, the occurrence of secretion and excretion and also responses including lachrymation, pilo-erection and respiratory patterns. Changes in gait,

posture and response to handling were also recorded [**Allan et al. 2007**]. In addition to observational study, body weights were recorded and blood and serum samples were collected from all the animals on the 7th day of the experiment to determine acute oral toxicity. The samples were analysed for total RBC, WBC, differential leucocytes count, haemoglobin percentage and biochemical parameters like ALKP, SGPT, SGOT, total cholesterol, triglycerides, creatinine, bilirubin, serum protein, tissue protein, malonaldehyde and reduced GSH activity. The animals were then sacrificed and were necropsied for any gross pathological changes. Weights of vital organs like liver, heart, kidney etc. were recorded [**Chanda et al. 2008**].

2.12. Statistical analysis

Soft agar colony formation, cell cycle, and Annexin V FITC experiments were performed in duplicates. *In-vivo* efficacy each group possessed six animal (n=6) and results are expressed as Mean±SD. For multiple comparisons each value was compared by one-way ANOVA following Dunnett test, Student t-test, and Tukey test in GraphPad Instat version 3.06. Comparisons are made relative to the untreated controls. p value<0.05 were considered significant. The statistical analysis was done using the Dunnett test. (**) indicates *p* values less than 0.01 and (*) denotes *p* values less than 0.05.

3. Results

3.1 Chemistry

Synthesis of fluorinated 2,3diarylindanone (**1**)

The synthetic strategy was as shown in Scheme 1, also described in our previous paper [**Saxena et al. 2008**, **Prakasham et al. 2012**]. It was little modified to get higher yields in several steps. Gallic acid was used as the starting substrate. Overall yield of fluorinated benzylidene indanone **1** was 14.29% in six synthetic steps starting with gallic acid.

Briefly, gallic acid was modified to trimethoxybenzoic acid methyl ester (**2**, 74%) using dimethyl sulphate in 40% aqueous alkali. It was reduced to 3,4,5-trimethoxybenzyl alcohol (**3**, 83%) by treating with lithium borohydride in THF at RT. This benzyl alcohol was oxidised with pyridinium chlorochromate in dry dichloromethane to get 3,4,5-trimethoxybenzaldehyde (**4**, 86%). Aldehyde **4** was treated with 3,4,5-trimethoxyacetophenone to get a hexamethoxychalcone (**5**, 95%) which underwent Nazarov's cyclization in trifluoroacetic acid in a sealed tube to get an indanone (**6**, 36%). Indanone **6** was treated with 4-fluorobenzaldehyde to get 2-benzylidene indanone **1** in 89% yield. The overall yield of fluorobenzylidene indanone **1** was 14.29% in six synthetic steps.

Scheme 1

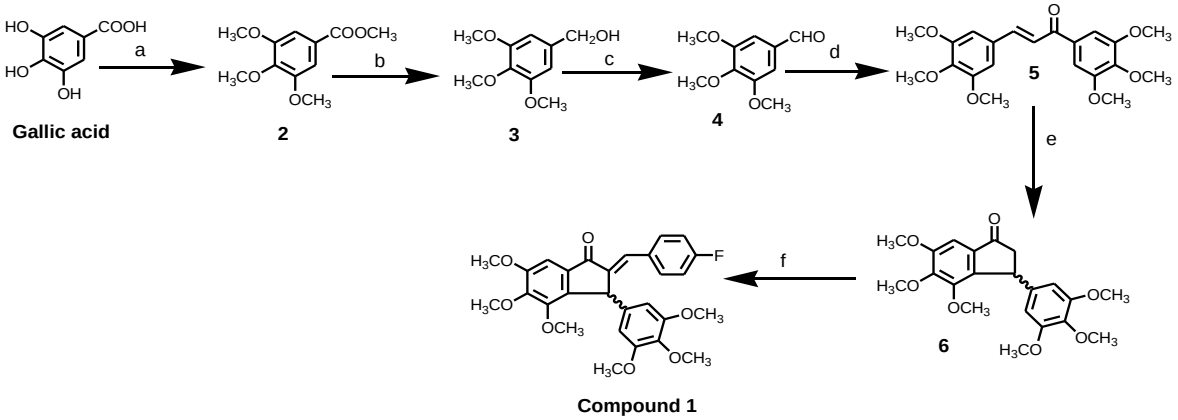

Reagents and conditions: a) Me_2SO_4, 30% Aqueous KOH, reflux, 3 h, 74%; b) $LiBH_4$, THF, RT, 83%; c) PCC, dry DCM, 10 ^oC-RT, 2 h, 86%, d) 7% KOH in MeOH, 3,4,5-trimethoxyacetophenone, RT, 6 h, 95%, e) TFA, 120 ^oC, 5 h, 36%, f) 3% KOH in MeOH, RT, 4 h, 89%.

3.2 Purity profile of compound 1 by UPLC

The purity of the fluorinated indanone **1**, was checked in Waters reversed phase UPLC system (USA) using PDA detector at 325 nm. The purity of the synthesized indanone **1** was found to be 99.70 %.

3.3 Cytotoxicity by Soft agar colony assay

To establish its *in-vitro* efficacy further, a soft agar colony assay was performed. The soft agar assay is considered as a gold standard assay for the transformed cell phenotype [**Rotem et al. 2015**]. Compound **1** significantly inhibited the colony forming ability of both MCF-7 (IC_{50}=27.10 µM) and MDA-MB-231 (IC_{50}=38.64 µM) cells (Table 1). This effect was more pronounced in MCF-7 cells as compared to MDA-MB-231. However, the cytotoxicity of fluorinated benzylidene in MCF-7 cells was lower than standard drug tamoxifen.

Table 1: Effect of compound **1** on percent colony formation in MCF-7 and MDA-MB-231 cells in soft agar after 24 h incubation.

MCF-7 Cells[d]					MDA-MB-231 cells[d]				
Compound	**Conc. µM**	**% Live cells**	**% Dead cells**	**IC_{50} µM**	**Compound**	**Conc. µM**	**% Live cells**	**% Dead cells**	**IC_{50} µM**
Control[a]	---	100	0	---	Control[b]	---	100	0	---
Tamoxifen	135	0	100	3.48	Tamoxifen	135	1.52±0.002	98.48	36.04
	54	0.19±0.02	99.81			54	36.99±0.02	63.01	
	27	4.96±0.03	65.04			27	58.77±0.04	41.23	
	13.5	19.42±0.13	80.58			13.5	74.17±0.01	25.83	
	4	42.13±0.61	57.87			4	85.98±0.01	14.02	
Compound **1**	101	2.85±0.05	97.15	27.10	Compound **1**	101	29.49±0.004	60.51	38.64
	40	30.95±0.2	69.05			40	51. 83±0.007	48.17	
	20	65.53±0.72	34.47			20	61.92±0.01	38.08	
	10	85.89±0.15	14.11			10	79.88±0.02	20.12	
	3	99.27±0.03	0.73			3	93.02±0.003	6.98	

** $p<0.01$ (Dunnett test), [a] total cells=41312; [b] total cells=3708, [d] no. of seeded cells=$5x10^4$ cells/mL, area of 60 mm plate=2826 mm^2.

3.4 Cell cycle analysis

In cell cycle analysis in MCF-7 cells, compound **1** exhibited G2/M phase arrest as depicted in figure 2. Flow cytogram clearly showed induction of apoptosis at all experimental concentrations (1.5µM-50µM). While in MDA-MB-231 cells, there was no significant change up to 10 µM concentrations. However, there were S phase and G2/M phase arrest at higher concentrations (20 µM and 50 µM). Here, apoptosis was induced only at 50 µM concentration.

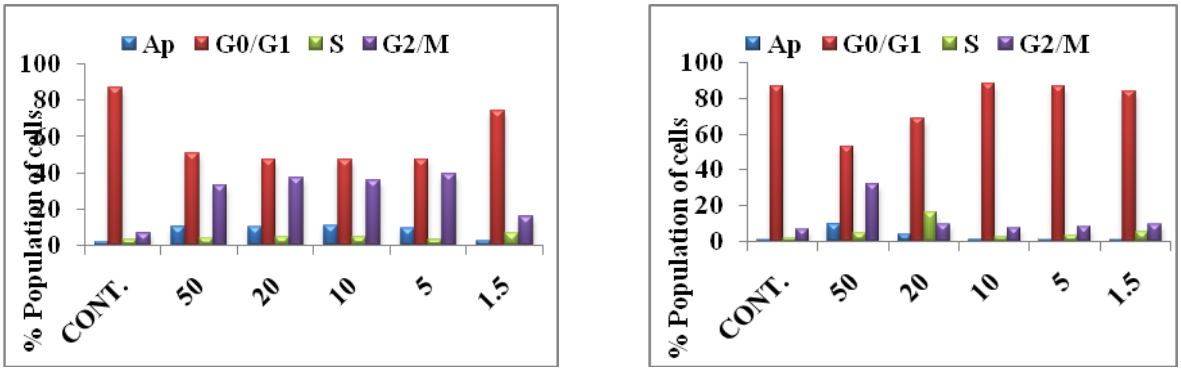

MCF-7 **MDA-MB-231**

Figure 2: Cell cycle of compound 1 in MCF-7 and MDA-MB-231 cells at various concentrations.

3.5 Apoptosis induction by Annexin V-FITC

As shown in figure 3, compound**1** induced early apoptosis at its IC_{50} concentration (0.68µM) in MCF-7 cells (4.2%) and late apoptosis (5%). 19.8% of cells were necrotic at this concentration. MDA-MB-231 cells treated with Compound **1** at its IC_{50} concentration also exhibited early apoptosis (0.7%) , late apoptosis (12.1%) and 15.1% showed necrosis.

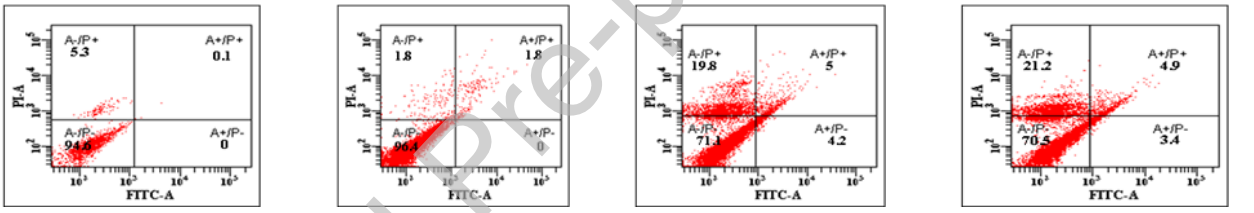

MCF-7: Control *½*IC_{50} (0.34 µM)* *IC_{50} (0.68 µM)* *2*IC_{50} (1.36 µM)*

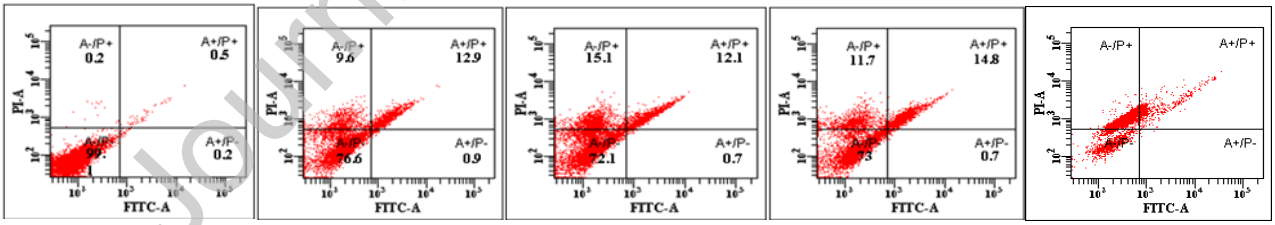

MDA-MB-231: Control *1/2IC_{50} (19.32 µM)* *IC_{50} (38.64 µM)* *2xIC_{50} (77.28 µM)* *Doxorubicin (1µg/mL)*

Fig. 3: Effect of compound **1** on Apoptosis Vs necrosis in MCF-7 and MDA-MB-231 cells (Annexin V-FITC)

3.6 Molecular docking studies

The calculated RMSD value between superimposed structure of redocked and β-Tubulin co-crystallised colchicine was found to be 0.63 which is well below cut off limit 2.0. A low RMSD value standardized the docking protocol. Here, colchicine binding site was taken for receptor-ligand interaction study. The binding site and its dimension are given under supplementary figure S1.

Colchicine redocking showed binding energy of -10.59 kcalmol^{-1} and form one hydrogen bond with amino acid residue VAL-181 (Figure S2). Analysis of docking results indicate the studied compound **1** exhibit docking binding energy of -8.54 kcalmol^{-1} which is comparable to the binding energy of positive control drug podophyllotoxin *i.e.*, -8.69 kcalmol^{-1}. Here, a docked pose with lowest estimated free energy of binding was selected as probable binding pose. Receptor-ligand complex insight analysis indicate compound **1** form number of non-covalent interactions namely van der Waals, halogen interaction, unfavourable acceptor-acceptor, pi-sigma, pi-sulfur and pi-alkyl (Figure 4A). Where binding pocket amino acid residues SER-178 and ALA-354 are involved in pi-sigma and pi-alkyl bonding with compound **1** aromatic rings. A halogen based weak interaction and an unfavourable acceptor-acceptor interaction was also observed between compound **1** amino acid residues VAL-315 and ASN-101 respectively (Table 2). Positive control podophyllotoxin is making four conventional hydrogen bonds with amino acid residues ASN-101, GLN-247, ASN-254 and ASN-258. Binding pose analysis indicate compound **1** trimethoxy and fluoride containing aromatic rings are shown to have similar orientation as that of colchicine aromatic rings with trimethoxy and oxygen based functional groups (Figure 4B).

Table **2**: Molecular docking based biding affinity results for positive control drug colchicine, podophyllotoxin and Compound **1** against anticancer drug target tubulin (PDB: 4O2B).

Name	**Docking binding energy kcal/mol**	**Binding site residues within 4Å region**	**Key amino acid residues**
Colchicine (co-crystallised ligand)	-10.59	Chain C: SER178, THR179, ALA180, VAL181 Chain D: CYS241, LEU242, LEU248, ALA250, ASP251, LYS254, LEU255, ASN258, MET259, THR314, VAL315, ALA316, ILE318, ASN350, LYS352, ALA354	VAL181
Podophyllotoxin	-8.69	Chain C: GLN11, ASN101, SER178, THR179, ALA180, VAL181, TYR224 Chain D: GLN247, LEU248, ASN249, ALA250, LYS254, LEU255, ASN258, LYS352, THR353	ASN101, LYS254, ASN258, GLN247
Compound 1	-8.54	Chain C: GLN11, ASN101, SER178, THR179, ALA180, VAL181, TYR224 Chain D: GLN-247, LEU248, ALA250, LEU 255, ASN258, MET259, VAL315, ALA316, ALA317, LYS352, THR353, ALA354,	SER178, ALA354

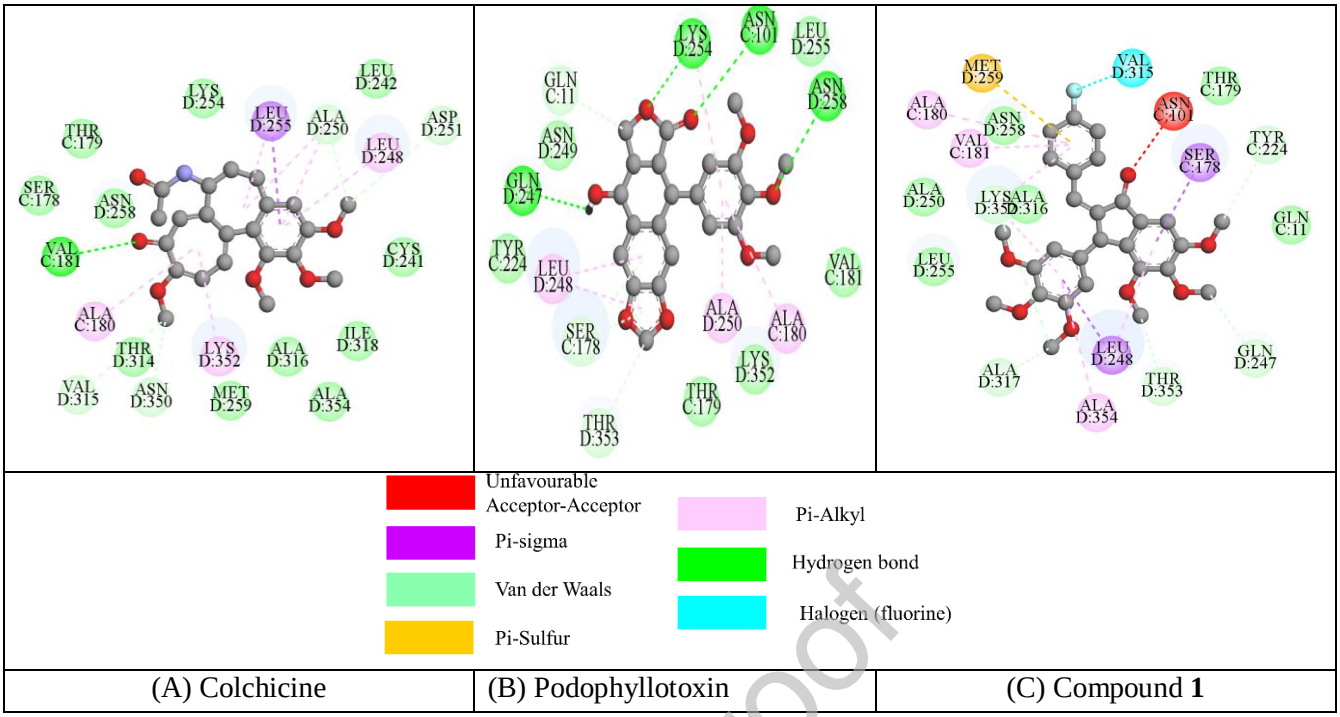

(A) Colchicine | (B) Podophyllotoxin | (C) Compound **1**

Fig. 4A: The 2D visualization of binding interactions between (A) colchicine, (B) podophyllotoxin and (C) Compound **1** and tubulin inhibitor binding pocket residues. The important interactions are highlighted with different colour dashed lines. The legend for colour code is given in the bottom.

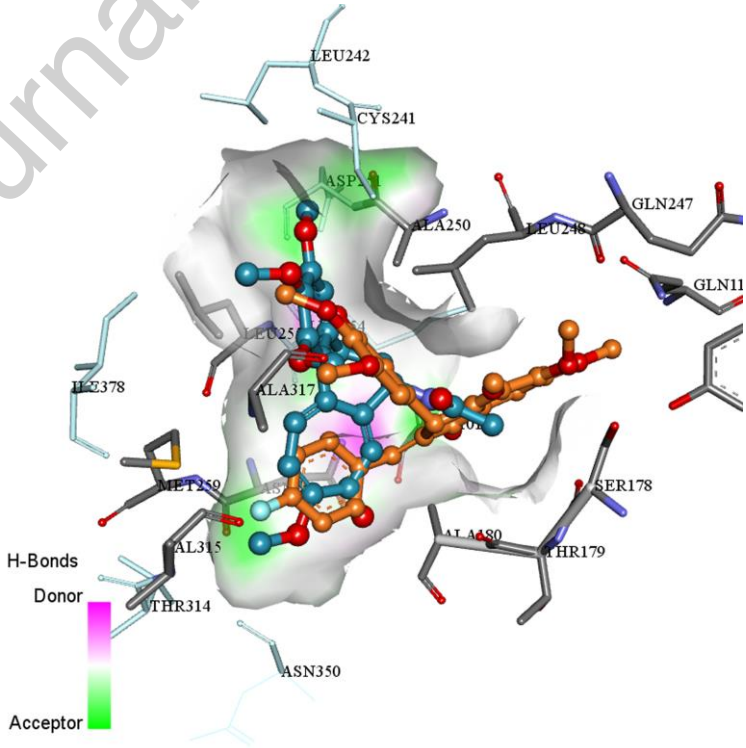

Figure 4B: A 3D representation of docked pose of compound **1** (orange) at β-Tubulin (PDB: 4O2B) colchicine binding site. Where ligands are shown in 'ball and stick' form and binding pocket residues are shown in 'stick' form with element based color coding (carbon; grey, oxygen; red, nitrogen; blue, sulphur; yellow and fluoride; sky blue). Compound **1** is shown in orange and colchicine is in blue colors ball and stick form.

3.7 *In silico* prediction of ADME properties

In *in-vivo* system, a drug candidate should reach to biological target in a sufficient concentration to exhibit desired pharmacological effect. There are several physicochemical parameters which play a crucial role in defining its success inside the body. A few physicochemical parameters like lipophilicity, water solubility, pharmacokinetics, Lipinski parameters, and PAINS (Pan-assay interference compounds) structure were predicted through SwissADME software (Table 3). Compound 1 exhibited satisfactory scores for various parameters. Figure 5 shows two dimensional bioavailability within the good bioavailability confined limits.

Table 3: Various druggability parameters of Podophyllotoxin Compound **1**.

Parameter	**Podophyllotoxin**	**Compd. 1**	**Acceptable range**	**Parameter**	**Podophyllotoxin**	**Compd. 1**	**Acceptable range**
Physicochemical properties				**Lipophilicity**			
Molecular formulae	C22H23O8	C28H27FO7	---	Log $P_{o/w}$	2.99	4.22	≤5
M. Wt.	414.41	494.51	≤500	**Pharmacokinetics**			
Rotable bonds	4	8	≤10	GI absorption	High	High	---
H-bond acceptors	8	8	≤10	BBB permeability	No	No	---
H-bond donors	1	0	≤5	P-gp substrate	No	Yes	---
Molar Refractivity	10.3.85	132.50	40-130	CYP1A2 inhibition	No	No	---
Sp3 hybridisation fraction	0.41	0.25	Not less than 0.25	CYP2C9/19 inhibition	No	Yes	---
TPSA	92.68Å^2	72.45Å^2	20 Å^2 to 130 Å^2	**Drug likeness**			
Water solubility				Lipinski rule	Yes, no violation	Yes, no violation	1 violation
Water solubility	81.2 µg/mL	0.49 µg/mL		Bioavailability score	0.55	0.55	moderate
Solubility class	Moderate	Poorly soluble	acceptable	**Medicinal chemistry**			
Log S	-3.71	-6.01	>-4	PAINS	No	No	

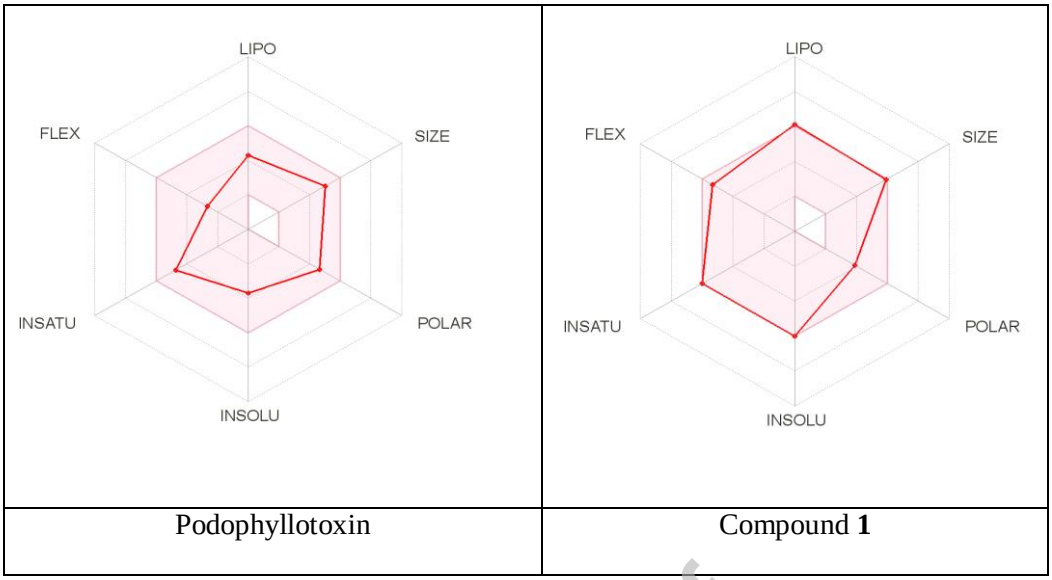

Podophyllotoxin	Compound **1**

Fig. 5: Two dimensional bioavailability radars of podophyllotoxin and compound **1**
(Six physicochemical properties are taken into account: lipophilicity, size, polarity, solubility, flexibility and saturation. The pink area represents the optimal range for each properties (lipophilicity: XLOGP3 between − 0.7 and + 5.0, size: MW between 150 and 500 g/mol, polarity: TPSA between 20 $Å^2$ and 130 $Å^2$, solubility: log S not higher than 6, saturation: fraction of carbons in the sp3 hybridization not less than 0.25, and flexibility: no more than 9 rotatable bonds. In this example, the compound is predicted not orally bioavailable, because too flexible and too polar.)

3.8 Antiangiogenic activity of benzylidene indanone 1 *via* VEGF and HIF-α inhibition

Compound **1** exhibited moderate antiangiogenic activity in MCF-7 cells (Figure 6). Compound **1** inhibited VEGF by 15-22% in concentration dependent manner. At its IC_{50} VEGF was inhibited by 17.2% in MCF-7 cells while doxorubicin induced 19-33% inhibition at its various concentrations. At its IC_{50} doxorubicin inhibited 33% of VEGF. Hypoxia inducible factor-α was inhibited by 28-40% by compound **1** in a dose-dependent manner. It inhibited 34.6% HIF-α at its IC_{50} (0.68 µM) while doxorubicin inhibited the same by 43.3% at its IC_{50} (5.83 µM).

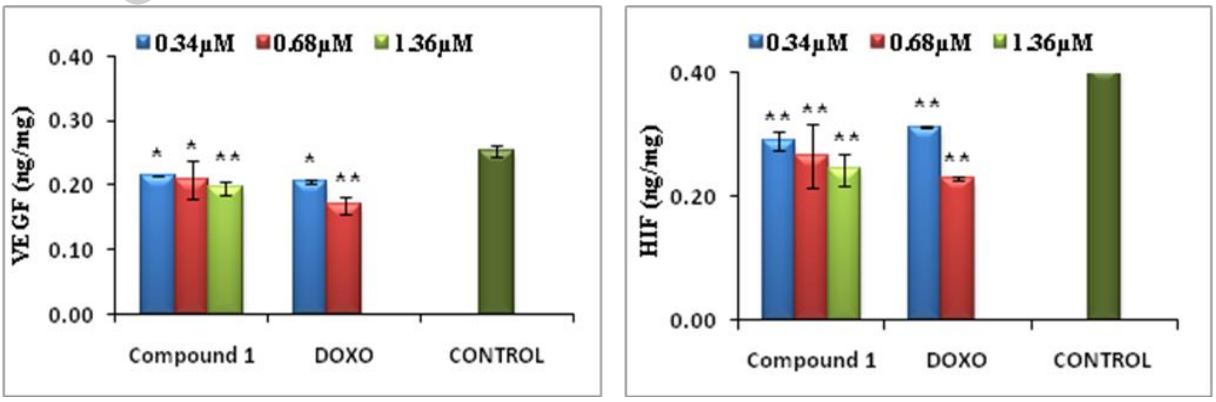

Fig. 6: Effect of Compound **1** on angiogenesis in MCF-7 cells VEGF and HIF at its various concentrations [Half IC_{50} (0.34 µM), IC_{50} (0.68 µM), and double IC_{50} (1.36 µM)] (Mean±SD; n=2, n*p<0.05 compared to control, ** p<0.01 compared to control)

3.9 *In-vivo* efficacy studies

In *in-vivo* efficacy experiment compound **1** showed moderate efficacy against C3H/Jax mice at 30 mg/kg oral dose. The results are presented in tables 4, 5 and 6. It reduced 48% tumour volume at 30 mg/kg oral dose. There was no significant improvement on further increasing doses to 60 and 120 mg/kg of compound **1**. There was no mortality and loss in weight of experimental animals throughout the experimental period. However, the T/C ratio was moderate i.e. 0.52.

Table 4: Average body weight (g) of mice during the experimental period (n=6)

Treatment	**Dose**	**Body weight (g)*** **			
		Day 1	**Day9**	**Day 18**	**Day 29**
Control	---	23.2±1.05	23.5±0.98	24.5±1.11	26.5±1.63
Compd. **1**	30 mg/kg, oral	24.6±2.27	24.8±2.18	25.0±2.47	27.4±2.72
Compd. **1**	60 mg/kg, oral	26.1±1.35	26.2±1.37	26.8±1.22	28.1±4.21
Compd. **1**	120 mg/kg, oral	26.6±1.46	26.3±1.44	26.7±1.78	27.9±1.65
Doxorubicin	2.5 mg/kg, i.v.	24.7±2.15	23.9±2.13	24.9±1.98	25.7±2.74

Mean±SD; ***p<0.01 compared to control

Table 5. Relative tumour volume (RTV) in various groups of experimental mice on treatment with compounds (n=6)

Treatment	**Dose**	**Relative Tumour Volume (RTV)***				**% Tumour reduction**	**% Survival**
		Day 1	**Day9**	**Day 18**	**Day 29**		
Control	---	1.00	5.98±1.63	17.32±4.14	43.83±14.35	---	100
Compd. **1**	30 mg/kg, oral	1.00	2.13±0.22	9.47±3.38	22.71±7.16	48.19±8.17	100
Compd. **1**	60 mg/kg, oral	1.00	2.97±0.33	12.40±5.43	34.50±18.51	21.29±11.21	100
Compd. **1**	120 mg/kg, oral	1.00	2.70±0.38	9.3±1.63	24.00±4.78	45.24±4.12	100
Doxorubicin	2.5 mg/kg, *i.v.*	1.00	1.92±0.62	4.84±3.06	8.87±3.01	79.76±4.17	100

Mean±SD; *p<0.05 compared to control

Table 6: T/C ratios for compound **1** at various doses and control drug doxorubicin (n=6)

Treatment	Dose	T/C[#, **]			
		Day 1	Day9	Day 18	Day 29
Control	---	1.00	---	---	---
Compd. **1**	30 mg/kg, oral	1.00	0.36±.04	0.55±0.17	0.52±0.16
Compd. **1**	60 mg/kg, oral	1.00	0.50±0.10	0.72±0.46	0.79±0.41
Compd. **1**	120 mg/kg, oral	1.00	0.46±0.06	0.53±0.09	0.55±0.09
Doxorubicin	2.5 mg/kg, i.v.	1.00	0.32±0.11	0.28±0.18	0.20±0.07

[#] Mean tumour volume of drug-treated mice/ mean tumour volume of control mice; Mean±SD; **p<0.01 compared to control

3.10 Safety studies by acute oral toxicity

There were no significant observational changes in, morbidity and mortality throughout the experimental period up to the dose level of 1000 mg/kg body weight of test compound **1**.

Blood and serum samples showed non-significant changes in all the parameters studied including total haemoglobin level, RBC count, WBC count, differential leucocyte-count, SGPT, ALKP, creatinine, triglycerides, albumin, serum protein, tissue protein, hepatic MDA and hepatic GSH activity (Table 7, 8 and Figure 8). However, SGOT was significantly increased in animals treated with the test drug at 1000 mg/kg body weight as compared to untreated control animals. Serum total cholesterol was significantly decreased in groups of animals treated with compound 1 at 5, 50 and 1000 mg/kg body weight as compared to the control group. A gross pathological study of drug-treated animals showed no changes in any of the organs studied including their absolute and relative weight (Figure 7). Therefore, the experiment showed that compound **1** is well tolerated by the Swiss albino mice up to the dose level of 1000 mg/kg body weight as a single acute oral dose. Overall, there were no observed adverse effect level (NOAEL) on experimental mice. Long term experiments need to be carried out to determine if any adverse effects are associated with -repeated exposure to compound **1** [**M.N. Ghosh 1984**].

Table 7. Effect of Compound **1** as a single acute oral dose at 5, 50, 300 and 1000 mg/kg body weight on body weight, haemogram and serum biochemical parameters in Swiss albino mice (Mean±SD; n=6).

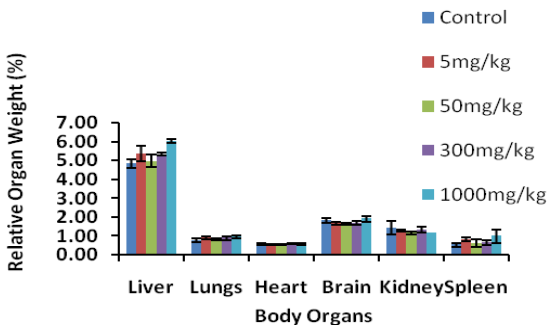

Fig. 7. Effect of Compound **1** as a single acute oral dose at 5, 50, 300 and 1000 mg/kg on absolute and relative organ weight in Swiss albino mice. (Mean±SD; n=6, Non significant changes were found compared to control).

Parameters	Dose of indanone **1** at mg/kg body weight as a single oral dose				
	Control	**5 mg/kg**	**50 mg/kg**	**300 mg/kg**	**1000 mg/kg**
Body weight (g)	20.63±3.08	17.42±1.45	21.09±1.13	21.68±2.65	19.12±3.20
SGPT (U/L)	9.92±2.68	9.30±8.73	7.62±3.17	8.95±6.59	7.19±0.08
SGOT (U/L)	15.99±7.78	17.21±3.67	15.87±8.17	33.39±6.34	24.07±1.71
ALKP (U/L)	258.24±48.21	261.57±65.31	267.65±33.11	257.24±88.01	246.52±121.87
Haemoglobin (g/dL)	11.41±2.30	11.95±1.02	11.45±1.62	12.11±1.78	11.49±0.15
Cholesterol (mg/dL)	88.45±26.79	56.33±7.23	68.81±12.41	57.98±11.21	44.83±13.30
Triglycerides (mg/dL)	60.61±16.58	67.24±13.68	45.26±22.99	55.46±19.43	43.94±2.95
Creatinine (mg/dL)	0.40±0.13	0.51±0.09	0.50±0.07	0.51±0.10	0.51±0.09
Albumin (mg/dL)	3.85±0.48	3.55±0.30	3.72±0.22	3.79±0.30	3.57±0.49
Serum protein (mg/mL)	0.15±0.01	0.12±0.02	0.13±0.03	0.12±0.02	0.14±0.01
Hepatic Tissue Protein (mg/ml; 10% w/v)	0.035±0.00	0.040±0.00	0.036±0.00	0.037±0.01	0.040±0.01
Hepatic MDA (nM/ mg protein)	0.031±0.009	0.026±0.009	0.027±0.008	0.035±0.020	0.045±0.018
Hepatic GSH (µM/mg protein)	0.21±0.025	0.20±0.023	0.21±0.022	0.22±0.043	0.18±0.052

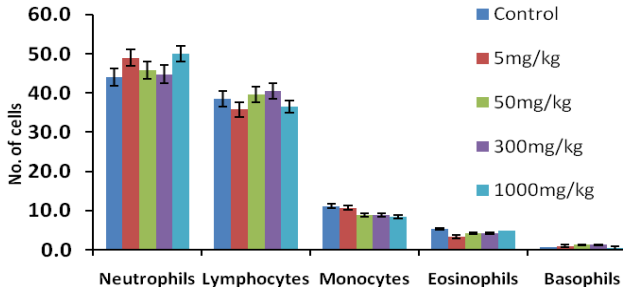

Fig. 8. Effect of Compound **1**as a single acute oral dose at 5, 50, 300 and 1000 mg/kg body weight on differential leucocytes counts in Swiss albino mice.(n=6, mean±SD, Non significant changes were found compared to control).

Table 8: The differential leucocytes count at different acute oral doses (n=6, percentage; mean±SD; Non significant changes were found compared to control).

Control	Neutrophils	Lymphocytes	Monocytes	Eosinophils	Basophils
	44.00±10.32	38.50±10.30	11.20±1.10	5.40±1.14	0.80±0.45
5mg/kg	49.00±4.69	35.80±4.21	10.80±1.30	3.40±1.14	1.00±0.71
50mg/kg	45.83±6.27	39.67±7.28	8.83±1.72	4.33±1.03	1.33±0.82
300mg/kg	44.83±15.60	40.50±13.69	9.00±2.00	4.33±1.86	1.33±1.37
1000mg/kg	50.00±1.41	36.50±2.12	8.50±0.71	5.00±0.00	0.50±0.71

4. Discussion

Breast cancer is a multifarious disease. Numerous biological targets have been established which has helped in developing newer cancer chemotherapeutics. The disease has been tackled to some extent with the help of the target specific anticancer drugs. However, there is still high morbidity and mortality due to this disease [**Nuzzolese et al. 2020**]. Affordability is one of the major concerns with the disease and researchers need to explore efficient, safer, and affordable cancer chemotherapeutics.

Over the years the unique attributes of fluorine has been well understood which yielded several useful fluorinated motifs [**N.A. Meanwell 2018**]. The judicious use of this element in a pharmacophore can affect the physical, biochemical, pharmacological, and pharmacokinetic properties beneficially [**Park et al., 2001**; **Shan & Westwell 2007**]. Its strong electronegativity, small size, and modest lypophilicity prefers it in drug design in recent years [**Jodnson et al. 2020**].

Benzylidene indanone **1** exhibited potent antiproliferative activity against hormone dependent breast cancer cell line MCF-7 with IC_{50} at 0.68 µM and microtubule destabilization with IC_{50} at 0.73µM [**Prakasham et al. 2012**]. Further, in soft agar colonisation assay it reduced the colony of MCF-7 cells with IC_{50} at 27.10 µM and MDA-MB-231 (IC_{50}=38.6 µM) cells. Soft agar colonisation

assay is used to confirm *in-vitro* cellular anchorage-independent growth. It is a well established assay to detect the tumorigenic potential of transformed cells and tumour suppressive effects on transformed cells [**Shin et al. 1975**]. Fluorinated indanone **1** significantly inhibited the proliferation of MCF-7 and MDA-MB-231 cells. Thus, compound **1**, may be effective against both hormone dependent (luminal) and hormone independent (basal) breast tumour cells *i.e.* a broad spectrum of breast tumour cells.

'Cell division cycle' deals with a series of coordinated events to replicate DNA in G1/S and to separate chromosomes to two daughter cells following mitotic phase [**Collins 1997**]. Cell cycle checkpoints ensure the accuracy of DNA replication and division [**Malumbres and Baracid 2009**]. The prime factor of cancer cells is to deregulate the cell cycle control [**Sher and Bartek 2017**]. Fluorinated indanone **1** effectively induced G2/M phase arrest in MCF-7 cells. However, in MDA-MB-231 cells G2/M phase arrest was effective only at higher concentration i.e. at 50µM. Microtubule dynamics modulators interfere during mitosis and induce cell cycle arrest at G2/M phase. Induction of cell cycle arrest in cancer cell lines constitutes one of the most prevalent strategies to stop or limit cancer spreading [**Hartwell and Weinert 1989**, **C.J. Sher 1996**].

The fluorinated indanone derivative **1** has exhibited antimitotic effect by destabilizing polymerisation of α/β-tubulin to microtubule polymer. Microtubules play an essential role in various cellular functions. Several studies indicate that their cellular actions are much more complex via protein-protein interactions and need to be understood [**Kaul et al. 2019**]. Docking studies demonstrated that it occupied colchicine binding pocket of β-tubulin. Both colchicine and compound **1** interacted with amino acid residue ALA316 which is considered crucial in inducing antimitotic effect. From competitive binding experiments, Burns *et al.* observed that residue β316 is closely involved in the hydrophobic interactions with 3,4,5-trimethoxy group of colchicine. Therefore, 3,4,5-trimethoxyphenyl is considered a crucial fragment in inducing antitubulin effect in the molecule [**Negi et al. 2015**].

Apoptosis and necrosis are two different processes causing cell death. Necrosis is caused by external factors to the cell and is considered to be a toxic process. Both these are natural barriers to restrict malignant cells from surviving and disseminating [**Su et al. 2015**]. Benzylidene indanone **1** induced apoptosis in the both MCF-7 and MDA-MB-231 cells. By induction of early and late apoptosis in cancer cells better therapeutic strategies can be developed for cancer treatment [**Cong et al. 2019**] .

Angiogenesis, a physiological process for the formation of new blood vessels plays a pivotal role in both normal embryonic and adult development [**Musumeci et al. 2012, Zhang et al. 2018**]. It

is considered as one of the six hallmarks of cancer [**Hanahan and Weinberg 2011**]. Uncontrolled proliferation of tumour cells requires high levels of nutrients and oxygen for rapid growth and development. These needs are met by tumour-induced angiogenesis which surprisingly is induced early in the multistage development of invasive cancers both in animal models and in humans [**Raica et al. 2009**]. The US FDA has approved several antiangiogenic drugs for clinical use in various types of cancer i.e. metastatic colorectal cancer, non-small lung cancer, metastatic breast cancer and metastatic renal cell carcinoma [**Carmeliet and Jain 2011**]. The fluorinated indanone **1** has exhibited moderate antiangiogenic activity by inhibiting VEGF and HIF-α significantly. VEGF plays a pivotal role in the process of angiogenesis for the formation of new blood vessels by modulating vascular network growth, vascular permeability and vessel cell survival [**Niu and Chen 2010**]. An imbalance in angiogenesis contributes to numerous malignant, inflammatory, ischaemic, infectious and immune disorders [**P. Carmeliet 2005**]. Therefore, the modulation of the VEGF-mediated angiogenic pathway is considered as an important target in anticancer drug development [**Niu and Chen 2010**]. Angiogenic inhibitors are relatively new class of anticancer drugs differing from classical cytotoxic drugs [**Kerbel and Folkman 2002**].

Based on our studies, it is evident that the antiproliferative effect of fluorinated indanone **1**, is through multitarget effect. Due to complexity of multifactorial diseases like triple negative breast cancer, single target drugs do not always exhibit satisfactory efficacy [**Zhou et al. 2019**]. However, pharmacokinetic effects and safety aspects should also be taken into consideration.

Fluorobenzylidene indanone **1** exhibited significant antitumour activity against EAC model. However, the effect on tumour reduction was not concentration dependent. The antitumour effect was evident from the doses i.e. 30 mg/kg (48% tumour reduction) and 120 mg/kg (45% tumour reduction). It seems that the dose response was saturated at 30 mg/kg and reaching pleatue as after that there was no improvement in the efficacy. In 60 mg/kg experimental error was more which exhibited poor activity. It is worth to mention that Ehrlich ascites carcinoma cells are considered difficult to break [**Beans and Kessel 1968**]. It is appraised as one of the most reliable models to assess preclinical efficacy of anticancer agents.

In safety studies benzylidene indanone **1** was well tolerated by the experimental mice and found to be safe up to 1000 mg/kg oral dose. Acute oral toxicity is a preliminary assessment of a lead compound after single or multiple exposures. It indicates adverse effects of the drug candidate in animal. There was some elevated level of SGOT at higher doses of benzylidene indanone **1**. It is quite possible with an anticancer compound when orally ingested. However, it was statistically non-

significant. Drug safety assessment is also termed as 'Pharmacovigilance' to focus on adverse drug reactions [**WHO 2002**]. It also gives as idea about risk-benefit profile of investigational drugs.

5. Conclusion

The fluorinated benzylidene indanone **1** exhibited potential antiproliferative activity through modulation of microtubule dynamics by occupying colchicine binding pocket. It also exhibited antiangiogenic effect by inhibiting VEGF and HIF-1α pathway. It was non-toxic and safe at much higher concentration than its efficacy dose. Overall, it shows moderate anticancer efficacy against breast cancer in rodent model. This investigational lead is under optimization for better efficacy.

6. Abbreviations

ER, Estrogen Receptor; ERα, Estrogen Receptor α-subtype; NCE, New Chemical Entity; HER-2, Human Epidermal Growth Factor Receptor-2; CDK, Cyclin Dependent Kinase; ESI-HRMS, Electrospray Ionisation-High Resolution Mass Spectrometry; UPLC, Ultra Pressure Liquid Chromatography; EAC, Ehrlich Ascites Carcinoma; US-FDA, United States Food and Drug Administration; VEGF, Vascular Endothelial Growth Factor; PAINS, Pan Assay Interference Compounds; IAEC, Institute Animal Ethical Committee; OECD, Organization for Economic Co-operation and Development ; SGOT, Serum Glutamate Oxaloacetic Transaminase; SGPT, Serum Glutamic Pyruvic Transaminase; ALKP, Alkaline Phosphatase

7. Declaration of competing interest

The authors declare no competing financial interest.

8. Acknowledgement

The study was financially supported from Department of Health Research, Govt. of India under GAP-432. Ms. Ankita Srivastava acknowledges to Department of Science and Technology, Govt. of India for her fellowship under WOS-A from KIRAN Division (GAP-407). Ms. Kaneez Fatima acknowledges CSIR for her Senior Research Fellowship. Chemical Central Facility of CSIR-CIMAP is duly acknowledged for Sophisticated Instrument support.

References

Allan, J.J., Damodaran, A., Deshmukh, N.S., Goudar, K.S., Amit, A., 2007. Safety evaluation of a standardized phytochemical composition extracted from *Bacopa monnieri* in Sprague-Dawley rats, Food Chem. Toxicol. 45, 1928–1937.

Baselga, J., Swain, S.M., 2010. CLEOPATRA: a phase III evaluation of pertuzumab and trastuzumab for HER2-positive metastatic breast cancer, Clin. Breast Cancer 10, 489–491.

Beans H.W., Kessel, R.G., 1968. Properties of the Ehrlich ascites tumour cell as determined by electron microscopy. Cancer Res. 28, 1944–1951.

Breast: Globocan: The global cancer observatory, March 2019.

Cancer: WHO factsheet, 12 September 2018.

Carmeliet, P., 2005. Angiogenesis in life, disease and medicine, Nature 438, 932-936.

Carmeliet, P., Jain, R.K., 2011. Molecular mechanisms and clinical applications of angiogenesis, Nature 473, 298-307.

Chanda, D., Shanker, K., Pal, A., Luqman, S., Bawankule, D.U., Mani, D.N., Darokar, M.P., 2008. Safety evaluation of Trikatu, a generic Ayurvedic medicine in Charles Foster rat, J. Toxicol. Sci. 34, 99-108.

Collins, K., Jacks, T., Pavletich, N.P.,1997. The Cell cycle and cancer, Proc. Natl. Acad. Sci. 94, 2776-2778.

Cong, H., Xu, L., Wu, Y., Qu, Z., Bian, T., Zhang, W., Xing, C., Zhuang, C., 2019. Inhibitor of Apoptosis Protein (IAP) Antagonists in Anticancer Agent Discovery: Current Status and Perspectives, J. Med. Chem. 62, 5750−5772.

Gan, P.P., Pasquier, E., Kavallaris, M., 2007. Class III β-tubulin mediates sensitivity to chemotherapeutic drugs in non-small lung cancer, Cancer Res. 67, 9356-9363.

Ghosh, M.N., 1984. In: Fundamentals of Experimental Pharmacology (1st Edition), Pp156, Scientific Book Agency, Kolkata.

Gupta, A., Kumar, B.S. , Negi, A.S., 2013. Current status on development of steroids as anticancer agents, J. Steroid Biochem. Mol. Biol. 137, 242-270.

Hanahan, D., Weinberg, R.A., 2011. Hallmarks of cancer: The next generation, Cell, 144, 646-674.

Hartwell, L.H., Weinert, T.A., 1989. Checkpoints: controls that ensure the order of cell cycle events, Science 246, 629–634.

Johnson, B.M., Shu, Y.Z., Zhuo, X., Meanwell, N.A., 2020. Metabolic and pharmacological aspects of fluorinated compounds. J. Med. Chem. 83, https://doi.org/10.1021/acs.jmedchem.9b01877

Kakuguchi, W., Kitamura, T., Kuroshima, T., Ishikawa, M., Kitagawa, Y., Totsuka, Y., Shindoh, M., Higashino, F., 2010. HuR knockdown changes the oncogenic potential of oral cancer cells, Mol. Cancer Res. 8, 520-528.

Kaul, R., Risinger, A.L., Mooberry, S.L., 2019. Microtubule-targeting drugs: more than antimitotics. J. Nat. Prod. 82, 680-685.

Kerbel, R., Folkman, J., 2002. Clinical translation of angiogenesis inhibitors, Nature Reviews Cancer 2, 727–739.

Looi, C.Y. , Arya, A., Cheah, F.K. , Muharram, B., Leong, K.H. *et al.*,2013. Induction apoptosis in human breast cancer cells via caspase pathway by vernodalin isolated from *Centratherum anthelminticum* (L) seeds. PLoS ONE 8, e56643.

Malumbres, M., Barbacid, M., 2009. Cell cycle, CDKs and cancer: a changing paradigm", Nature Reviews Cancer. 9, 153–166.

Meanwell, N.A., 2018. Fluorine and fluorinated motifs in the design and application of bioisosteres for drug design. J. Med. Chem. 61, 5822-5880.

Menezes, J.C.J.M.D.S., 2017. Aryilidene indanone scaffold: medicinal chemisty and structure activity relationship. RSC Advances 7, 9357-9372.

Musumeci, F., Radi, M., Brullo, C., Schenone, S., 2012. Vascular endothelial growth factor (VEGF) receptors: drugs and new inhibitors, J. Med. Chem. 55, 10797−10822.

Negi, A.S., Gautam, Y., Alam, S., Chanda, D., Luqman, S., Sarkar, J., Khan, F., Konwar, R., 2015. Natural antitubulin agents: Importance of 3,4,5-trimethoxyphenyl Fragment, Bioorg. Med. Chem. 23, 373-389.

Niu, G., Chen, X., 2010. Vascular Endothelial Growth Factor as an Anti-angiogenic Target for Cancer Therapy. Current Drug Targets 18, 1000-1017.

Nowsheen, S., Aziz, K., Panayiotidis, M.I., Georgakilas, A.G., 2012. Molecular markers for cancer prognosis and treatment: Have we struck gold? Cancer Letters 327, 142–152.

Nuzzolese, I., Montemurro, F., 2020. Attrition in metastatic breast cancer: a metric to be reported in randomised clinical trials? The Lancet Oncology 21, 21-24.

Park, B.K., Kitteringham, N.R., O'Neill, M., 2001. Metabolism of fluorine containing drugs. Ann. Rev. Pharmacol. Toxicol. 41, 443-470.

Petrica, L., Ursoniu, S., Gadalean, F., Vlad, A., Gluhovschi, G., Dumitrascu, V., Vlad, D., Gluhovschi, C., Velcioy, S., Bob, F., Matusz, P., Secara, A., Simulescu, A., Popescu, R., 2017. Urinary podocyte-associated mRNA levels correlate with proximal tubule dysfunction in early diabetic nephropathy of type 2 diabetes mellitus, Diabetol. Metab. Syndr. 9, 31.

Phelan, J.P., Reen, F.J., Dunphy, N., Connor, R.O., Gara, F.O., 2016. Bile acids destabilise HIF-1α and promote anti-tumour phenotypes in cancer cell models, BMC Cancer 16, 476.

Prakasham, A.P., Saxena, A.K., Luqman, S., Chanda, D., Kaur, T., Gupta, A., Yadav, D.K., Chanotiya, C.S., Shanker, K., Khan, F., Negi, A.S., 2012. Gallic acid based benzylidene indanones as anticancer agents, Bioorg. Med. Chem. 20, 3049-3057.

Raica, M., Cimpean, A.M., Ribatti, D., 2009. Angiogenesis in pre-malignant conditions, Eur. J. Cancer 45, 1924–1934.

Reen, F.J., Flynn, S., Woods, D.F., Dunphy, N., Chroinin, M.N., Mullane, D., Stick, S., Adams, C., O'Gara, F., 2016. Bile signalling promotes chronic respiratory infections and antibiotictolerance, Sci. Rep. 6, 29768

Riccardi, C., Nicoletti, I., 2006. Analysis of apoptosis by propidium iodide staining and flow cytometry, Nature Protocols 1, 1458-1461.

Rotem, A., Janzer, A., Izar, B., Ji, Z., Doench, J.G., Garraway, L.A., Struhl, K., 2015. Alternative to the soft-agar assay that permits high throughput drug and genetic screens for cellular transformation, Proc. Natl. Acad. Sci. 112, 5708-5713.

Samavat, H., Kurzer, M.S., 2015. Estrogen metabolism and breast cancer, Cancer Letters 356, 231–243.

Saxena, H.O., Faridi, U., Srivastava, S., Kumar, J.K., Darokar, M.P. , Luqman, S., Chanotiya, C.S., Krishna V., Negi, A.S., Khanuja, S.P.S., 2008. Gallic acid based indanone derivatives as anticancer agents. Bioorg. Med. Chem. Lett. 18, 3914-3918.

Shah, P., Westwell, A.D., 2007. The role of fluorine in medicinal chemistry. J. Enz. Inhib. Med. Chem. 22, 527-540.

Shimizu, Y., Furuya, H., Greenwood, P.B., Chan, O., Dai, Y., Thornquist, M.D., Goodison, S., Rosser, C.J., 2016. A multiplex immunoassay for the non-invasive detection of bladder cancer. J. Transl. Med. 14, 31.

Shin, S.I., Freedman, V.H., Risser, R., Pollack, R., 1975.Tumorigenicity of virus-transformed cells in nude mice is correlated specifically with anchorage independent growth *in vitro*, Proc. Natl. Acad. Sci. 72, 4435-4439.

Sher, C.J., 1996. Cancer cell cycles, Science 274, 1672-1677.

Sher, C.J., Bartek, J., 2017. Cell cycle: Targeted cancer therapies, Annual Rev Cancer Biol. 1, 41-57.

Su, Z., Yang, Z., Xu, Y., Chen, Y., Yu, Q., 2015. Apoptosis, autophagy, necroptosis, and cancer metastasis. Mol. Cancer 14, 48.

WHO., 2002. The Importance of Pharmacovigilance, Safety Monitoring of medicinal products. World Health Organization.

Zhang, Y., Chen, Y., Zhang, D., Wang, L., Lu, T., Jiao, Y., 2018. Discovery of Novel Potent VEGFR-2 Inhibitors Exerting Significant Antiproliferative Activity against Cancer Cell Lines, J. Med. Chem. 61, 140-157.

Zhou, J., Jiang, X., He, S., Jiang, H., Feng, F., Liu, W., Sun. H., Qu. 2019. Rational design of multitarget-directed ligands: strategies and emerging paradigm. J. Med. Chem. 62, 8881-8914.

.....

Credit author statement

Ankita Srivastava, Eram Fatima, & Aastha Singh —chemical synthesis

Kaneez Fatima & Suaib Luqman-Soft agar analysis, cell cycle, Antiangiogenesis, annexin V experiments

Arjun Singh & Debabrata Chanda- Acute oral toxicity

Aparna Shukla & Feroz Khan- Molecular docking studies

Karuna Shanker-Purity profile

Arvind S. Negi- Design & synthesis, manuscript preparation, overall planning, responsibility etc.

Table, Figure and Scheme Legends

Table 1: Effect of compound **1** on percent colony formation in MCF-7 and MDA-MB-231 cells in soft agar after 24h incubation. (no. of seeded cells=5x10^4 cells/mL, area of 60mm plate=2826mm^2)

Table 2: Molecular docking based biding affinity results for positive control drug colchicine, podophyllotoxin and Compound **1** against anticancer drug target tubulin (PDB: 4O2B).

Table 3: Various druggability parameters of Podophyllotoxin Compound **1**.

Table 4: Average body weight (g) of mice during the experimental period (n=6, mean±SD; ***p<0.01, compared to control).

Table 5: Relative tumour volume (RTV) in various groups of experimental mice on treatment with compounds (n=6, Mean±SD; *p<0.05, compared to control).

Table 6: T/C ratios for compound **1** at various doses and control drug doxorubicin (n=6) (n=2, mean±SD; ** p<0.01 compared to control)

Table 7: Effect of Compound **1** as a single acute oral dose at 5, 50, 300 and 1000 mg/kg body weight on body weight, haemogram and serum biochemical parameters in Swiss albino mice . (n=6, mean±SD; Non significant changes were found compared to control).

Table 8: The differential leucocytes count at different acute oral doses (n=6, percentage; Mean±SD)

Figure 1: Some of the clinical drugs being used against breast cancer

Figure 2: Effect of compound **1** at different concentrations on cell division cycle of; (A) in MCF-7 cells; (B) in MDA-MB-231 cells

Figure 3: Effect of compound **1** on Apoptosis Vs necrosis at different concentrations by Annexin V-FITC assay, (A) in MCF-7 cells, and (B) MDA-MB-231 cells

Figure 4A: The 2D visualization of binding interactions between (A) colchicine, (B) podophyllotoxin and (C) Compound **1** and tubulin inhibitor binding pocket residues. The important interactions are highlighted with different colour dashed lines. The legend for colour code is given in the bottom.

Figure 4B: Figure 4B: A 3D representation of docked pose of compound **1** (orange) at β-Tubulin (PDB: 4O2B) colchicne binding site. Where ligands are shown in 'ball and stick' form and binding pocket residues are shown in 'stick' form with element based color coding (carbon; grey, oxygen; red, nitrogen; blue, sulphur;

yellow and fluoride; sky blue). Compound **1** is shown in orange and colchicine is in blue colors ball and

stick form.

Figure 5 : Two dimensional bioavailability radars of podophyllotoxin and compound **1**

(Six physicochemical properties are taken into account: lipophilicity, size, polarity, solubility, flexibility and saturation. The pink area represents the optimal range for each properties (lipophilicity: XLOGP3 between − 0.7 and + 5.0, size: MW between 150 and 500 g/mol, polarity: TPSA between 20 and 130 A2, solubility: log S not higher than 6, saturation: fraction of carbons in the sp3 hybridization not less than 0.25, and flexibility: no more than 9 rotatable bonds. In this example, the compound is predicted not orally bioavailable, because too flexible and too polar.)

Figure 6: Effect of Compound **1** on angiogenesis at its various concentrations (Half IC_{50}, IC_{50} and double IC_{50}) in MCF-7 cells, (A) VEGF, and (B) HIF-α

(n=2, mean±SD; *p<0.05 compared to control, ** p<0.01 compared to control)

Figure 7: Effect of Compound **1**as a single acute oral dose at 5, 50, 300 and 1000 mg/kg on absolute and relative organ weight in Swiss albino mice. (n=6, mean±SD; non significant changes were found compared to control).

Figure 8: Effect of Compound **1**as a single acute oral dose at 5, 50, 300 and 1000 mg/kg body weight on differential leucocytes counts in Swiss albino mice. (n=6, percentage; mean±SD; Non significant changes were found compared to control).

Scheme 1: Reagent and conditions i) Me_2SO_4, 40% KOH, for 30 min: 0-10^{o}C, afterwards reflux 3h, 74%; ii) $LiBH_4$, dry THF, 60^{o}C/RT, 3h, 83%; iii) DCM, PCC, RT, 3h, 86%; iv) 3,4,5-trimethoxyacetophenone, 3% KOH in MeOH, RT, 5h, 95%; v) Trifluoroacetic acid, sealed/pressure tube, 110^{o}C, 5h, 32%; vi) 7% KOH in MeOH, RT, 3h, 89%.

……

Table 1

MCF-7 Cells[c]					MDA-MB-231 Cells[c]				
Compound	**Conc. µM**	**% Live cells**	**% Dead cells**	**IC_{50} µM**	**Compound**	**Conc. µM**	**% Live cells**	**% Dead cells**	**IC_{50} µM**
Control[a]	---	100	0	---	Control[b]	---	100	0	---
Tamoxifen	135	0	100	3.48	Tamoxifen	135	1.52±0.002	98.48	36.04
	54	0.19±0.02	99.81			54	36.99±0.02	63.01	
	27	4.96±0.03	65.04			27	58.77±0.04	41.23	
	13.5	19.42±0.13	80.58			13.5	74.17±0.01	25.83	
	4	42.13±0.61	57.87			4	85.98±0.01	14.02	
Compound **1**	101	2.85±0.05	97.15	27.10	Compound **1**	101	29.49±0.004	60.51	38.64
	40	30.95±0.2	69.05			40	51. 83±0.007	48.17	
	20	65.53±0.72	34.47			20	61.92±0.01	38.08	
	10	85.89±0.15	14.11			10	79.88±0.02	20.12	
	3	99.27±0.03	0.73			3	93.02±0.003	6.98	

** $p<0.01$ (Dunnett test), [a] total cells=41312; [b] total cells=3708, [c] no. of seeded cells=$5x10^4$ cells/mL, area of 60 mm plate=2826 mm^2.

Table 2

Name	Docking binding energy kcal/mol	Binding site residues within 4Å region	Key amino acid residues
Colchicine (co-crystallised ligand)	-10.59	Chain C: SER178, THR179, ALA180, VAL181 Chain D: CYS241, LEU242, LEU248, ALA250, ASP251, LYS254, LEU255, ASN258, MET259, THR314, VAL315, ALA316, ILE318, ASN350, LYS352, ALA354	VAL181
Podophyllotoxin	-8.69	Chain C: GLN11, ASN101, SER178, THR179, ALA180, VAL181, TYR224 Chain D: GLN247, LEU248, ASN249, ALA250, LYS254, LEU255, ASN258, LYS352, THR353	ASN101, LYS254, ASN258, GLN247
Compound 1	-8.54	Chain C: GLN11, ASN101, SER178, THE179, ALA180, VAL181, TYR224 Chain D: GLN247, LEU248, ALA250, LEU255, ASN258, MET259, VAL315, ALA316, ALA317, LYS352, THR353, ALA354	SER178, ALA354

Table 3

Parameter	Podophyllotoxin	Compd. 1	Acceptable range	Parameter	Podophyllotoxin	Compd. 1	Acceptable range
Physicochemical properties				**Lipophilicity**			
Molecular formulae	C22H23O8	C28H27FO7	---	Log $P_{o/w}$	2.99	4.22	≤5

M. Wt.	414.41	494.51	≤500	**Pharmacokinetics**			
Retable bonds	4	8	≤10	GI absorption	High	High	---
H-bond acceptors	8	8	≤10	BBB permeability	No	No	---
H-bond donors	1	0	≤5	P-gp substrate	No	Yes	---
Molar Refractivity	10.3.85	132.50	40-130	CYP1A2 inhibition	No	No	---
Sp3 hybridisation fraction	0.41	0.25	Not less than 0.25	CYP2C9/19 inhibition	No	Yes	---
TPSA	92.68Å^2	72.45Å^2	20 Å^2 to 130 Å^2	**Drug likeness**			
Water solubility				Lipinski rule	Yes, no violation	Yes, no violation	1 violation
Water solubility	81.2 µg/mL	0.49 µg/mL		Bioavailability score	0.55	0.55	moderate
Solubility class	Moderate	Poorly soluble	acceptable	**Medicinal chemistry**			
Log S	-3.71	-6.01	>-4	PAINS	No	No	

Table 4

Treatment	Dose	Body weight (g)			
		Day 1	Day9	Day 18	Day 29
Control	---	23.2±1.05	23.5±0.98	24.5±1.11	26.5±1.63
Compd. **1**	30 mg/kg, oral	24.6±2.27	24.8±2.18	25.0±2.47	27.4±2.72
Compd. **1**	60 mg/kg, oral	26.1±1.35	26.2±1.37	26.8±1.22	28.1±4.21
Compd. **1**	120 mg/kg, oral	26.6±1.46	26.3±1.44	26.7±1.78	27.9±1.65
Doxorubicin	2.5 mg/kg, i.v.	24.7±2.15	23.9±2.13	24.9±1.98	25.7±2.74

Mean±SD; ***p<0.01, compared to control).

Table 5

Treatment	Dose	Relative Tumour Volume (RTV)			% Tumour reduction	% Survival
		Day9	Day 18	Day 29		
Control	---	5.98±1.63	17.32±4.14	43.83±14.35	---	100
Compd. **1**	30 mg/kg, oral	2.13±0.22	9.47±3.38	22.71±7.16	48.19±8.17	100
Compd. **1**	60 mg/kg, oral	2.97±0.33	12.40±5.43	34.50±18.51	21.29±11.21	100
Compd. **1**	120 mg/kg, oral	2.70±0.38	9.3±1.63	24.00±4.78	45.24±4.12	100
Doxorubicin	2.5 mg/kg, *i.v.*	1.92±0.62	4.84±3.06	8.87±3.01	79.76±4.17	100

Mean±SD; *p<0.05, compared to control).

Table 6

Treatment	Dose	T/C$^{\#}$		
		Day9	Day 18	Day 29
Control	---	---	---	---

Parameters	Dose of Indanone **1** at mg/kg body weight as a single oral dose			
Compd. **1**	30 mg/kg, oral	0.36±.04	0.55±0.17	0.52±0.16
Compd. **1**	60 mg/kg, oral	0.50±0.10	0.72±0.46	0.79±0.41
Compd. **1**	120 mg/kg, oral	0.46±0.06	0.53±0.09	0.55±0.09
Doxorubicin	2.5 mg/kg, i.v.	0.32±0.11	0.28±0.18	0.20±0.07

T/C[#] Mean tumour volume of drug-treated mice divided by the mean tumour volume of control mice;

Mean±SD; [**] p<0.01, compared to control).

Table 7.

	Control	5 mg/kg	50 mg/kg	300 mg/kg	1000 mg/kg
Body weight (g)	20.63±3.08	17.42±1.45	21.09±1.13	21.68±2.65	19.12±3.20
SGPT (U/L)	9.92±2.68	9.30±8.73	7.62±3.17	8.95±6.59	7.19±0.08
SGOT (U/L)	15.99±7.78	17.21±3.67	15.87±8.17	33.39±6.34	24.07±1.71
ALKP (U/L)	258.24±48.21	261.57±65.31	267.65±33.11	257.24±88.01	246.52±121.87
Haemoglobin (g/dL)	11.41±2.30	11.95±1.02	11.45±1.62	12.11±1.78	11.49±0.15
Cholesterol (mg/dL)	88.45±26.79	56.33±7.23	68.81±12.41	57.98±11.21	44.83±13.30
Triglycerides (mg/dL)	60.61±16.58	67.24±13.68	45.26±22.99	55.46±19.43	43.94±2.95
Creatinine (mg/dL)	0.40±0.13	0.51±0.09	0.50±0.07	0.51±0.10	0.51±0.09
Albumin (mg/dL)	3.85±0.48	3.55±0.30	3.72±0.22	3.79±0.30	3.57±0.49
Serum protein (mg/mL)	0.15±0.01	0.12±0.02	0.13±0.03	0.12±0.02	0.14±0.01
Hepatic Tissue Protein (mg/ml; 10% w/v)	0.035±0.00	0.040±0.00	0.036±0.00	0.037±0.01	0.040±0.01
Hepatic MDA (nM/ mg protein)	0.031±0.009	0.026±0.009	0.027±0.008	0.035±0.020	0.045±0.018
Hepatic GSH (µM/mg protein)	0.21±0.025	0.20±0.023	0.21±0.022	0.22±0.043	0.18±0.052

Table 8

	Neutrophils	Lymphocytes	Monocytes	Eosinophils	Basophils
Control	44.00±10.32	38.50±10.30	11.20±1.10	5.40±1.14	0.80±0.45
5mg/kg	49.00±4.69	35.80±4.21	10.80±1.30	3.40±1.14	1.00±0.71
50mg/kg	45.83±6.27	39.67±7.28	8.83±1.72	4.33±1.03	1.33±0.82
300mg/kg	44.83±15.60	40.50±13.69	9.00±2.00	4.33±1.86	1.33±1.37
1000mg/kg	50.00±1.41	36.50±2.12	8.50±0.71	5.00±0.00	0.50±0.71

Figure 1

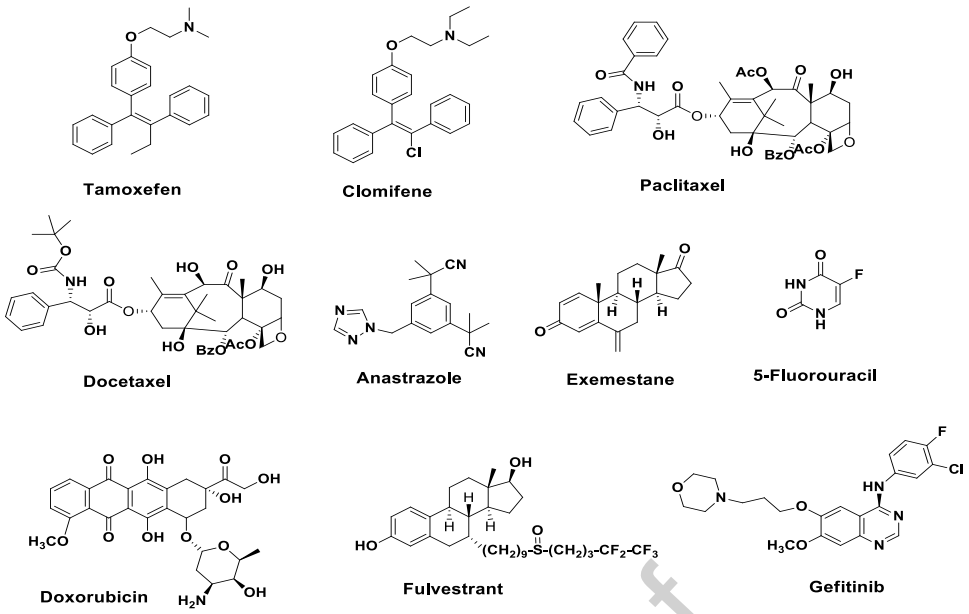

Figure 2

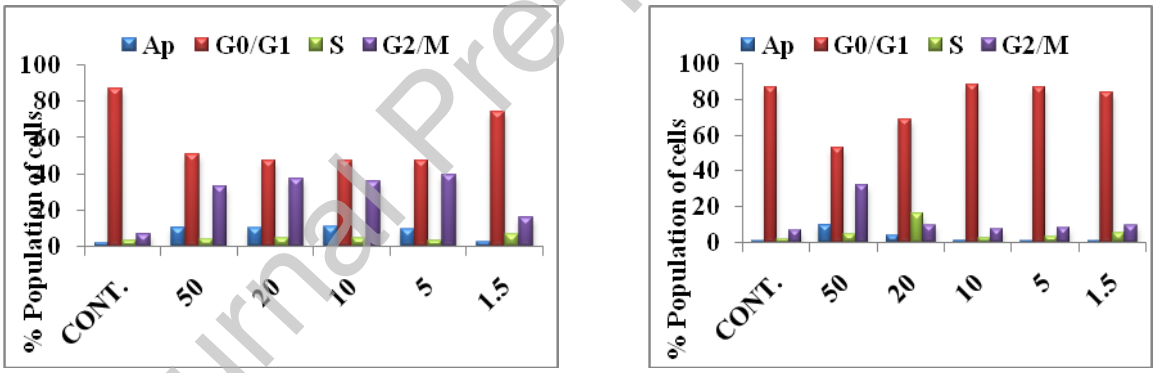

MCF-7 MDA-MB-231

Figure 3

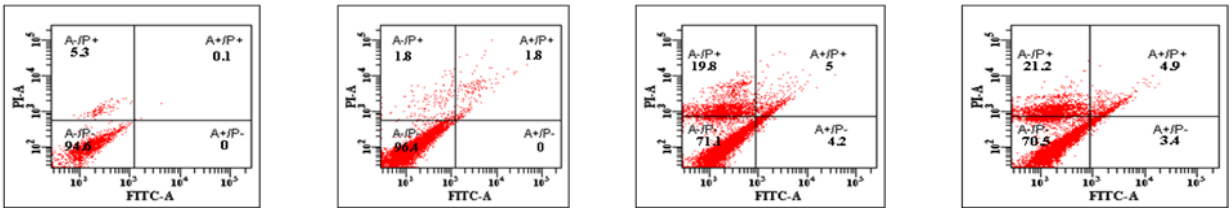

MCF-7: Control *½*IC$_{50}$ (0.34 µM)* *IC$_{50}$ (0.68 µM)* *2*IC$_{50}$ (1.36 µM)*

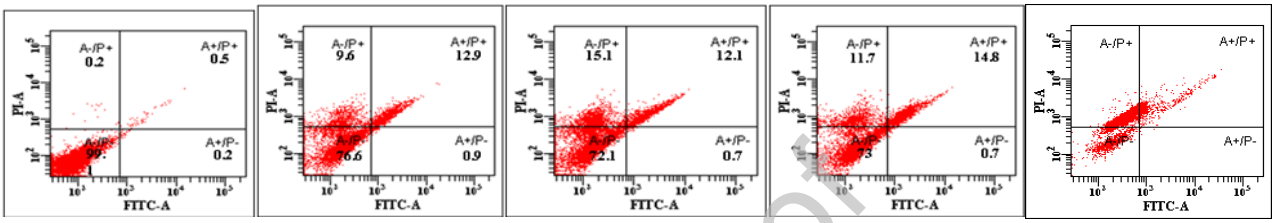

MDA-MB-231:Control *1/2IC$_{50}$ (19.3µM)* *IC$_{50}$ (38.6µM)* *2xIC$_{50}$ (77.2 µM)* *Doxorubicin (1µg/mL)*

Figure 4A

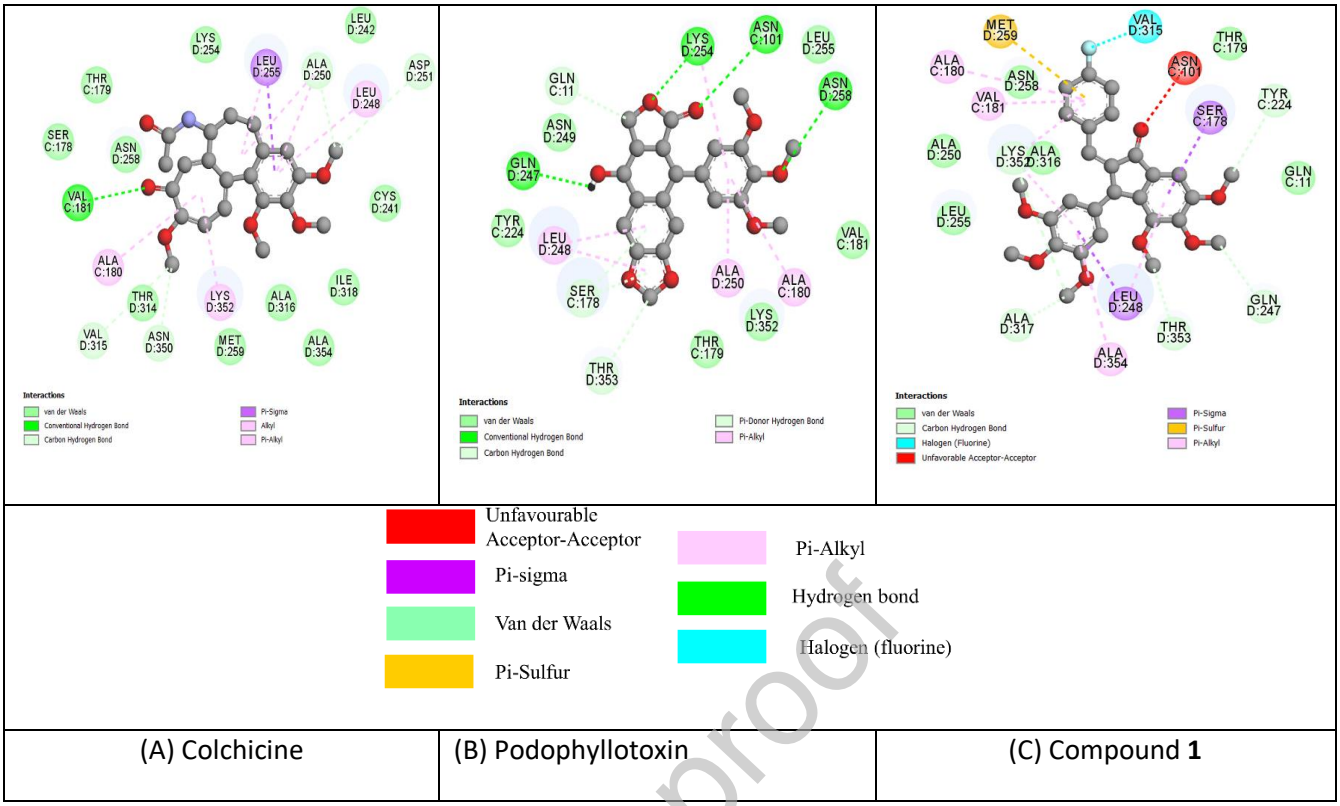

(A) Colchicine | (B) Podophyllotoxin | (C) Compound **1**

Figure 4B:

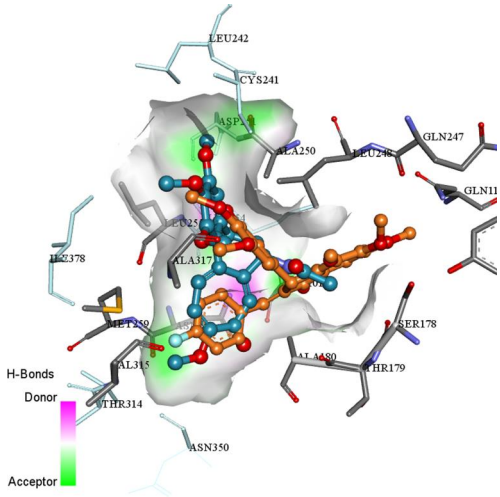

Figure 5

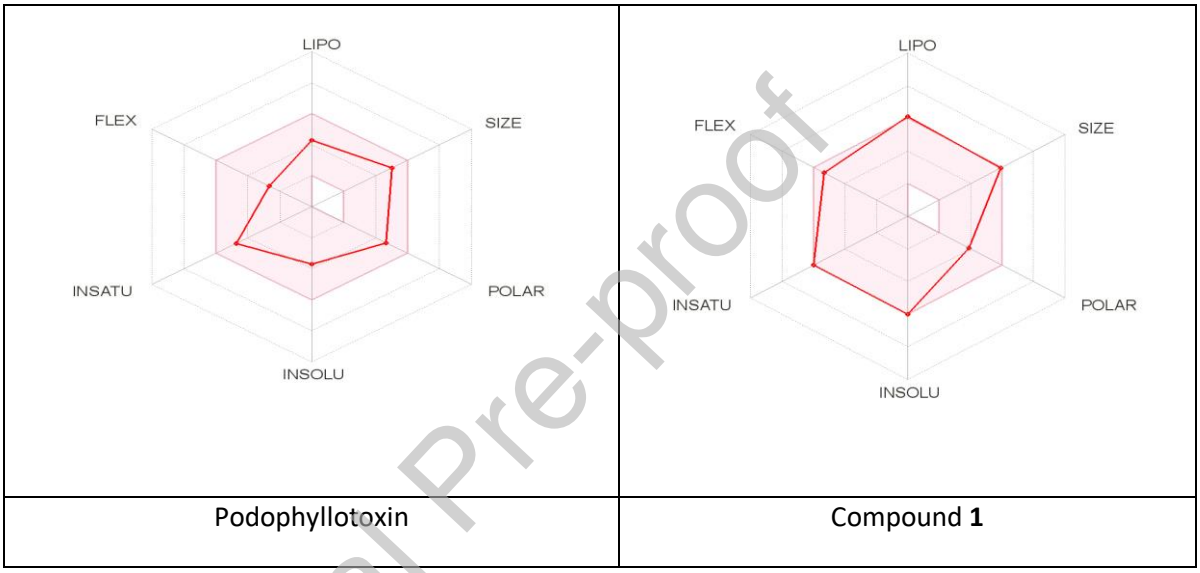

Podophyllotoxin	Compound **1**

Figure 6

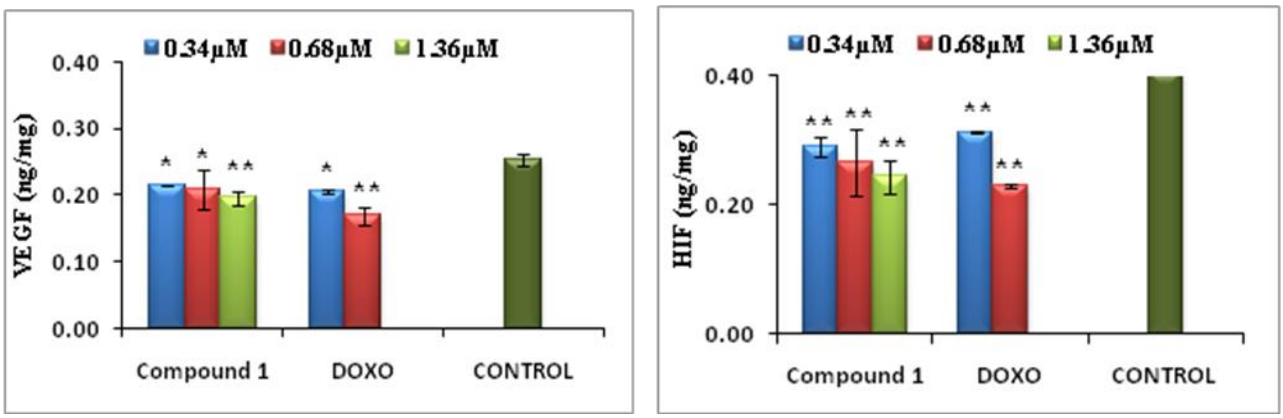

(A) **(B)**

Figure 7

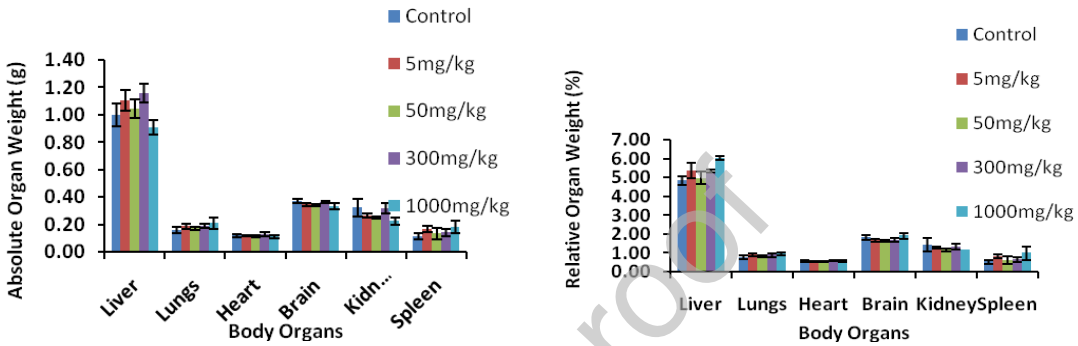

Figure 8

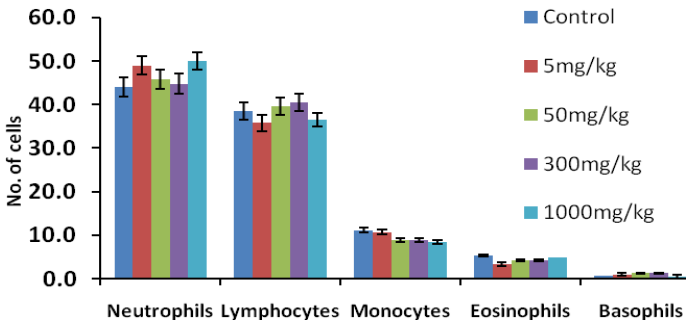

Scheme 1

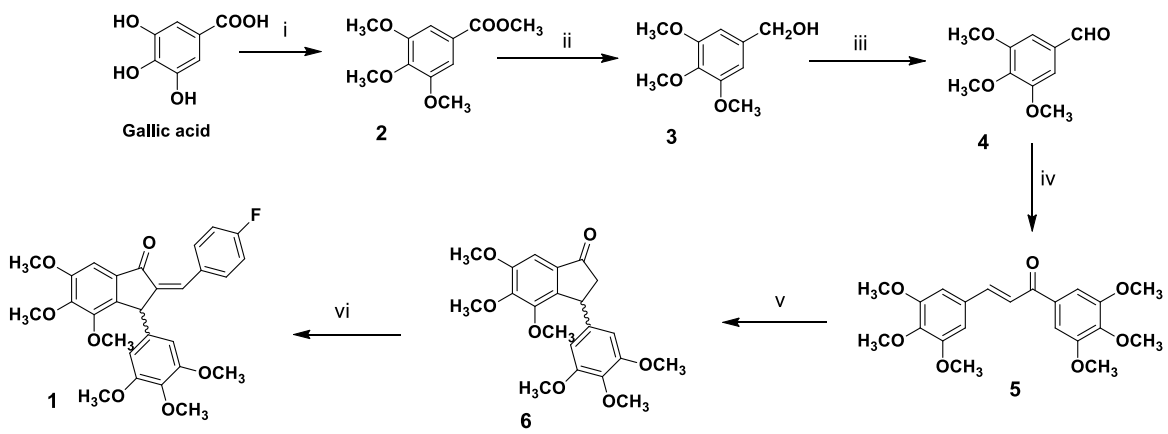

.....

Graphical Abstract

To create your abstract, type over the instructions in the template box below.
Fonts or abstract dimensions should not be changed or altered

Fluorinated benzylidene indanone exhibits antiproliferative activity through modulation of microtubule dynamics and antiangiogenic activity

Leave this area blank for abstract info.

Ankita Srivastava, Kaneez Fatima, Eram Fatima, Arjun Singh, Aastha Singh, Aparna Shukla, Suaib Luqman, Karuna Shanker, Debabrata Chanda, Feroz Khan, Arvind S. Negi